Accepted Manuscript

Journal of the Geological Society

Transport of mafic magma through the crust and sedimentary basins: Jameson Land, East Greenland

Christian Haug Eide, Nick Schofield, John Howell & Dougal A Jerram

DOI: https://doi.org/10.1144/jgs2021-043

To access the most recent version of this article, please click the DOI URL in the line above. When citing this article please include the above DOI.

Received 30 March 2021
Revised 12 October 2021
Accepted 19 October 2021

Supplementary material at https://doi.org/10.6084/m9.figshare.c.5670470

Transport of mafic magma through the crust and sedimentary basins: Jameson Land, East Greenland

Christian Haug Eide[1*], Nick Schofield[2], John Howell[2], and Dougal A, Jerram[3,4]

[1] Department of Earth Science, University of Bergen, Box 7803, 5020 Bergen, Norway

[2] School of Geosciences, Meston Building, University of Aberdeen, Aberdeen AB24 3UE, UK

[3]Centre for Earth Evolution and Dymanics (CEED), University of Olso, Postbox 1028 Blindern N-0315 Oslo, Norway

[4]DougalEARTH Ltd. Solihull, UK.

* Correspondence: christian.eide@uib.no

Running head: Transport of mafic magma through the crust

14 188 words, 98 references, 0 tables, 13 figures.

Supplementary materials:

DR1: Uninterpreted and un-warped version of seismic line in Fig. 4

DR2: Spreadsheet showing thickness of sills and width of dykes in study area.

DR3: Assumptions and calculations of magma volume in southern Sill Complex in Jameson land Basin

1. Abstract:

Igneous sheet-complexes transport magma through the crust, but most studies have focused on single segments of the magma-transport-system or have low resolution. In the Jameson Land Basin in East Greenland, reflection-seismic data and extensive outcrops give unparalleled constraints on mafic intrusions down to 15 km. This dataset shows how sill-complexes develop and how magma is transported from the mantle through sedimentary basins. The feeder zone of the sill-complex is a narrow zone below basin, where a magmatic underplate body impinges on thinned crust. Magma was transported through the crystalline crust through dykes. Seismic data and published geochemistry indicate magma was supplied from a magmatic underplate, without perceptible storage in crustal magma-chambers and crustal assimilation. As magma entered the sedimentary basin, it formed distributed, bowl-shaped sill-complexes throughout the basin. Large magma volumes in sills (4-20 times larger than the Skaergaard Intrusion), and few dykes highlight the importance of sills in crustal magma-transport. On scales smaller than 0.2 km, host-rock lithology, and particularly mudstone tensile strength-anisotropy, controls sill-architecture in the upper 10km of the basin, whereas sills are bowl-shaped below the brittle-ductile transition zone. On scales of kilometres and towards basin margins, tectonic stresses and lateral lithological changes dominate architecture of sills.

2. Introduction

Sill-complexes are interconnected magma conduits that are broadly parallel to stratigraphy, transgress upwards and transfer magma through the crust and in certain cases to eruption (e.g. Lorenz & Haneke 2004; Cartwright and Møller-Hansen, 2006; Jaxybulatov et al 2014; Schofield et al 2015; Eide et al 2017). Interconnected sill-complexes appear to be the primary way in which mafic magma is transported through sedimentary basins, in contrast to more viscous silicic magmas which are more likely to form plutons (Cartwright and Hansen, 2006; Muirhead et al 2014; Schofield et al 2015; Magee et al 2016; Haafez et al 2017; Svensen et al., 2018; Magee et al 2019). Studies on sill-complexes are often focused on data types that highlight specific segments of the magma transport pathway (reflection seismic data, outcrops of sill-complexes, active volcanoes, geochemistry) or have low resolution (earthquake data, seismic tomography, refraction seismic data). Insights into basic principles of crustal magma transport and intrusion geometries can be gained from outcrop examples (e.g. Hansen et al., 2011; Schofield et al., 2012; Eide 2017), seismic data (e.g. Planke et al., 2015; Magee et al 2016; Schofield et al., 2017), and through analogue and numerical modelling studies (e.g. Galland et al., 2012; Kavanagh et al 2017; Walker & Gill 2020), yet linking the complete plumbing architecture from deep in the crust to the surface is a challenge (Jerram and Bryan 2015). Understanding the geometry of the magma transport system and physical controls on development of sill-complexes is not only valuable to map out the route of magma within upper crustal and basin settings, understanding the propagation and architecture of sill-complexes is also important to interpret earthquake (e.g. Sigmundson et al 2010) and ground deformation data (e.g Pedersen and Sigmundsson, 2004; Galland 2012; Magee et al 2017) related to volcanic unrest. Another area where understanding intrusion networks is important, is for utilization of geologic resources in intruded basins (e.g. hydrocarbons, groundwater, mineral resources, geothermal heat; e.g. Senger et al 2017, MacDonald et al 2001; Hayman et al 2021 and Elders et al 2014, respectively).

The Jameson Land Basin in East Greenland (Fig 1) is an onshore basin that contains a large amount of mafic igneous intrusions. This basin offers a unique opportunity to understand magma transport

through the crust and sedimentary basin on scales from centimetres to tens of kilometres because 1) about 3 km of post-emplacement erosion (Mathiesen et al 2000, Hansen et al 2001) has dissected the mafic intrusions leading to extensive unvegetated outcrops where dykes (subvertical igneous sheets) and sills (broadly layer-concordant igneous sheets) can be readily investigated in large 10's km scale outcrops (Figs 2, 3), 2) there is a well-constrained stratigraphy due to widespread outcrops and decades of surface and subsurface geological investigations (e.g. Surlyk et al 1973; Dam & Surlyk 1998, Ahokas et al 2014; Eide et al 2016, 2017, 2018; Guarneri et al 2017; Brethes et al 2018), 3) extensive refraction seismic surveys have been performed directly offshore from the outcrops, leading to good control on the crustal structure and P-wave velocities in the basin (Fig. 1B; Weigel et al 1995; Mandler & Jokat 1998), and 4) because an onshore 2D grid of reflection seismic data (Fig. 2A) makes it possible to investigate both structure of the basin and distribution of intrusions at depth.

Integration of available data from the Jameson Land Basin allows us to bridge the observational gap between field and seismic studies in three dimensions, investigate a mafic volcanic plumbing system in an area that is 60x120 km in extent and more than 15 km deep, and link those observations to deeper crustal structure from refraction seismic data extending down to c. 30 km. Because the thick cover of shallow level intrusions and lava flow sequences, which reflect seismic energy and can commonly make sub-basalt imaging difficult (e.g. Ziolkowski et al 2003; Hautot et al., 2007; Jerram et al., 2009; Eide et al 2018) is eroded in the Jameson Land Basin, the study site offers a rare opportunity of a window to image deeper intrusions and link them to both occurrences of the same intrusions in outcrop, and to the overall crustal structure. No studies have yet investigated at all these different datasets from the Jameson Land Basin together, and little is therefore known about intrusion geometries throughout the basin, what controls these geometries, and what it means for our understanding of magma transport in sedimentary basins.

In this contribution, we show that two sill-complexes shaped as nested bowls occur in the Jameson Land Basin and that at least the most-well imaged of these are fed from a narrow zone along the axis of the basin. We investigate the basin-scale controls on the shape of these sill-complexes, and what

these insights tell us about controls on magma-transport and sill emplacement through sedimentary basins. In particular, this study offers insights into how magma behaves as it propagates from the crystalline crust into a sedimentary basin, and how igneous intrusions are controlled by lithology, far-field stresses and position within a sedimentary basin. The goals of this paper are to (1) present the structure of the Jameson Land Basin and the igneous intrusions within it, (2) investigate the controls on the architecture of the Jameson Land intrusive complex at shallow to deep crustal levels, and (3) discuss how the observations from the Jameson Land Basin might be relevant to understanding mafic sill-complexes in general.

3. Geological history of the Jameson Land Basin

The Jameson Land Basin in East Greenland is a N-S trending, c. 15 km deep (Figs. 1A, 4; Mandler & Jokat 1998), basin that formed after collapse of the Caledonian orogeny. The stratigraphic succession in the Jameson Land Basin consists of three main packages (e.g. Guarneri et al 2017) which are discernible in the seismic data (Fig 4A): (1) An upper unit in the uppermost 1.5 S TWT (c. 2 km) characterized by a gently concave upwards, un-faulted succession overlying (2) a middle unit with rotated fault blocks and associated growth wedges (0.7-1.5 km thick), and (3) a poorly imaged lower part below the growth wedges c 10 km thick. Stratigraphic interpretation in the upper two units is straightforward because the different seismic units crop out and can be compared to units in the geological map (Fig. 2; e.g. Bengaard & Henriksen 1982; Pedersen et al 2013; Guarneri et al 2017; Brethes et al 2018). The upper unit corresponds to the Late Triassic – Early Cretaceous post-rift succession, the middle unit corresponds to the syn-rift Triassic Pingo Dal Formation, and the lower unit consists of undifferentiated pre-rift deposits and basement. It is worth noting that what is termed "pre-rift" here are deposits of several pre-Triassic rift- and post-rift events, but none of these can be differentiated in the present seismic data. The boundary between the pre-rift sediments and basement is seldom possible to pick confidently, but the top of a basement block is imaged in

the seismic data towards the eastern part of the basin (Fig. 5), and this interpretation is supported by extensive outcrop, aeromagnetic and electromagnetic data (Guarneri et al 2017). Post-Triassic rift episodes in the East Greenland left few marks in the Jameson Land Basin, and deposits younger than the Cretaceous are eroded as the basin has been subject to c 3 km of erosion since the Eocene (Mathiesen et al 2000, Hansen et al 2001).

The opening of the North Atlantic gave rise to the North Atlantic Igneous Province and to emplacement of large amounts of igneous rocks along what is now the North Atlantic margins during the Palaeocene and Eocene (e.g. Saunders et al 1997; Hansen et al 2009; Brooks, 2011; Larsen et al 2014; Horni et al 2017). Opening of the North Atlantic and sea-floor spreading on the Ægir spreading ridge (Fig. 1A) commenced at c 55 Ma. Several kilometres of flood basalts were also emplaced in central East Greenland at the same time as onset of sea-floor spreading, constrained to 55-53.5 (e.g Larsen et al 2014). Importantly, around this time significant mafic underplating of the crust occurred along East Greenland. This magma was supplied from the nearby palaeo-Iceland plume, which fed the flood basalt succession (Hopper et al., 2003; Voss and Jokat, 2007; Voss et al., 2009). This high-density underplated region and the mantle beneath it represents the original source-regions for the melt generation.

The studied sills and dykes in outcrops in the Jameson Land Basin are interconnected, geochemically high-Ti tholeiitic basalts dated to 53 Ma using Ar-Ar and palaeomagnetism and are interpreted to have ben emplaced in a single intrusive episode based on the geochemistry (Hald & Tegner, 2000). Thus, the studied intrusives slightly postdate the main flood basalts in East Greenland, and they are not geochemically similar to any preserved flood basalts in the area (Hald & Tegner, 2000). The outcropping intrusions were emplaced into Jurassic sandstones and mudstones at a depth of 3 km during maximum burial. This estimate is based on analysis of vitrinite reflectance data, apatite fission track data, and reconstructions of eroded stratigraphy (Mathiesen et al, 2000; Hansen et al 2001). This implies that the intrusions in surface outcrops today were emplaced at c 3 km depth. The intrusions at c 15 km depth today, which are imaged in the seismic reflection data in Jameson Land, were emplaced at ~ 18 km. These constraints are taken into account for our models for sill

emplacement presented later in this contribution. Any volcanoes, lava sequences and shallow intrusions (which may have intruded into un-cemented, overlying host-rocks) have now been eroded from the study area.

A change in plate movement in the Oligocene led to northward propagation of the North Alantic, a ridge-jump from the Ægir to the Kolbeinsey ridge, and separation of the Jan Mayen Microcontinent from Liverpool Land during 40-25 Ma (Fig 1A; Talwani & Eldholm 1977; Mjelde et al 2008; Gaina et al 2009). This event is believed to have led to emplacement of a small number of narrow alkaline dykes that cross-cut the studied tholeiitic basalts which have been reported in the Jameson Land (Hald & Tegner, 2000; Eide et al 2017), and also many places in central East Greenland (Brooks, 2011; Larsen et al 2014). It should be noted that older alkaline magmatic events do occur that are coincident in age with the NAIP *sensu stricto*, and seem to be spatially linked with the Jan Mayen fracture zone (ref Hafeez et al. 2017), so without absolute dating the exact age of the alkali basalts rocks remains unresolved.

4. Dataset and methods

The study area comprises the areas of Jameson Land covered by 2D seismic data and a virtual outcrop dataset (Fig 2A). Sedimentological logs were acquired in a field campaign in 2012 (Eide et al 2016).

The virtual outcrop dataset (Fig. 3; available for study at https://v3geo.com/model/61) was acquired from the sea-cliffs on the west side of Hurry Inlet using helicopter-mounted lidar scanning (Buckley et al 2008). It has a resolution of c. 7 cm and is 32 km long and c 400 m high. The data was visualized using LIME (Buckley et al 2019), and 22 km of this dataset is shown in this paper (Fig. 3A) as the rest has only minor amounts of intrusions. Igneous intrusions in this outcrop are clearly visible as up to 17 m thick, most commonly 10 m thick, dark-coloured resistant rocks emplaced within the Early Jurassic sandstones and mudstones (Fig. 3, Eide et al 2016, 2017, for additional statistics on sill and dyke geometries see spreadsheet in DR2). These thicknesses measurements are created by

measuring the vertical thickness of all outcropping sills every 1 km along the outcrop, and the width of every exposed dyke. The geometries of igneous intrusions in the virtual outcrop were used to generate synthetic seismograms that help to constrain interpretation of seismic data in the area (Fig 3B,C). These seismograms were presented in, and are reproduced from, Eide et al (2018).

The studied 2D seismic data was acquired by Atlantic Richfield Company (ARCO) from 1986 to 1989 in a hydrocarbon exploration campaign targeting onshore East Greenland (Larsen & Marcussen 1992), and are available through the Geological Survey of Denmark and Greenland (GEUS). Most of these seismic lines were acquired using a dynamite source, leading to deep penetration, high frequencies preserved to great depth (dominant frequencies from sill reflectors at 15-20 Hz at 5 s TWT, c. 14 km depth), and in general good imaging of sills and locally also sedimentary geometries. The lines are spaced 5-10 km apart (Fig. 2A). P-wave velocities are taken from refraction seismic experiments published by Mandler & Jokat (1998; Fig 1B,C). The studied host-rocks have been subject to c. 3 km of erosion since deposition, and therefore show a high P-wave velocities at the surface and a low velocity-depth gradient (Fig 1C; Mandler & Jokat, 1998). The observed velocities are consistent with patterns observed in deep wells on the Norwegian Continental shelf when 3 km of erosion are accounted for (Fig 1C). In seismic data (Fig 4), sills appear as high-amplitude, hard-kick (increase in acoustic impedance) reflectors, which correspond to seismic responses where sills have a red coloured upper reflection and a blue-coloured bottom reflection with the chosen colour scale (Fig 5C). The reflections from interpreted sills are in the vast majority of cases *tuned*, which means they are so thin that they do not give separate reflections from top and base (Fig. 5C) and their thickness at depth can therefore not be confidently estimated.

It must also be noted that it is not possible to seismically distinguish between the "high-titanium-basalts" (emplaced at c. 53 Ma), and the cross-cutting alkali basalts (assumed to be emplaced later at c 30 Ma) (Hald & Tegener 2000). However, less than 10% of the sills investigated by Hald & Tegner (2000) consist of alkali basalts, indicating that these are rare compared to the main, high-titanium basalts.

Map data from the seamless digital 1: 500 000 scale geological map of Greenland (Pedersen et al 2013) has been used in this study (Fig. 2A), and this data is also available through GEUS (see

http://maps.greenmin.gl/geusmap/?mapname=greenland_portal)

5. Results

5.1 Architecture of sills and dykes in outcrops

The igneous intrusions in the Jameson Land Basin are well-exposed in the sea cliffs on the west side of Scoresby Sund (Fig 2), where they can be observed as dark, transgressive intrusive rocks commonly 10 m thick, within the lighter Jurassic host rock (Fig. 3). Dykes and sills are mainly interconnected, and sills in many cases turn into dykes and vice versa (Fig 3A, D, E). Sills are mainly emplaced within weak lithologies: On the large scale as sills are preferentially emplaced within the large regional mudstone beds, within more restricted mudstones overlying flooding surfaces, and within poorly cemented sandstones (Fig. 3A, F; Eide et al 2016). This is true both on the scale of hundreds of meters to several kilometres (Fig. 3A), but also on the scale of cm to m, as thin sill "*splays*" exploit mudstone-draped cross-bed foresets in tidal dunes (Fig. 3G). 84% of the sills (by area of outcropping sills on fig. 3A) occur in mudstone-dominated lithologies (Eide et al 2017). This indicates that mudstones must have a fundamental control on the architecture of sill-complexes. This will be discussed below.

Host-rocks mainly consist of thinly bedded (cm's to dm's) sandstones and mudstones in the southern part of the outcrop, and thick (10s of m) sandy packages interbedded with regional mudstones (1-20 m thick) in the N part (Fig. 3A).

Most sills are *stepped sills* in the sense that they are horizontally segmented by *broken bridges* (*sensu* Schofield et al 2012) and longer transgressive dykes, and the segments are generally vertically offset and show an upwards-to-the-north trend (green dashed lines in Fig. 3A; Fig 3D). The length of the sill segments increases from c. 0.2 km in the southern part of the outcrop (Fig. 3D), through c. 1 km

in the middle part, to c. 6 km in the N part (Fig. 3F). This increase in segment spacing coincides with an increase in sandstone content towards the north in the outcrop (Fig. 3A). This indicates that the segment spacing and jog height is strongly controlled by host-rock properties, which is discussed in detail later. In most of the outcrop, two sills occur within 50 m vertical distance from each other, these occasionally cross-cut each other. Thus, the studied outcrop exposes part of a *sill-complex*.

5.2 Basin-scale architecture of sills

In the seismic data from the Jameson Land Basin, the intrusions occur as high amplitude reflections that show hard-kicks (i.e. an increase in acoustic impedance), that can be seen to transgress stratigraphy and show layer-parallel, layer-parallel oblique and rarely saucer-shaped geometries in the uppermost parts (Fig 4). These reflections are interpreted as the same mafic igneous intrusions that are seen in outcrop because of their similarity to igneous intrusions in seismic data elsewhere (e.g. Cartwright and Huuse, 2003; Reynolds et al., 2017; Eide et al 2018), documented presence in the basin (Larsen & Marcussen 1992; Eide et al 2017; Larsen 2018), and attitude towards outcrops where they are observed and sampled (Figs 3, 4). Some of these reflections are clearly stepped and are thus interpreted as stepped sills such as the sills observed in outcrop (e.g. Fig. 3D). Other high-amplitude reflectors at greater depths are clearly oblique, and it is unclear whether these represent truly oblique igneous sheet intrusions or if they are highly transgressive stepped sills, as it is not possible to distinguish between these two geometries in lower quality seismic data because of limited lateral resolution (compare Figs 3B and 3C). Based on the lack of truly oblique sheets in the outcrop (Fig. 3A), we speculate that these dipping seismic reflectors are mainly highly transgressive stepped sills. Because of this, and because of the low dip of oblique high-amplitude reflections (commonly 6°, maximum 15°), we refer to all broadly subhorizontal subsurface igneous sheets as sills.

Sills are present at all levels in the basin (i.e. from 0-15 km depth), and no particular depth intervals or stratigraphic intervals appear to have accumulated a greater proportion of sills than other intervals (Fig 6). It should be pointed out that the seismic resolution decreases with depth, so it is

possible that a constant amount of intrusions imaged in seismic data might indicate an increase in amount of intrusions with depth. Both in outcrop (Fig. 3) and in similar basins around the North Atlantic (e.g. Faroe-Shetland Basin, Mark et al 2018), mafic sill intrusions preferentially exploit mudstone beds. This implies that mud-dominated lithologies occur at many levels throughout the basin-fill.

Sills observed in the seismic data are generally flat-lying and concordant to stratigraphy in the upper 4 km of the basin, and in the central parts of the basin at great depth (4-6 S TWT, c. 9-15 km). Towards the basin margins, sill reflectors are oblique with regard to stratigraphy, and transgress upwards away from two distinct zones at the base of the basin, one area in the north and one area in the south of the basin (Figs. 4, 5A, 6). This indicates that there are two main sill-complexes in the Jameson Land Basin, and that these have two distinct feeder zones at the base of the basin (Fig. 7). We term these the Southern and Northern Sill-complexes.

For the S Sill-complex, the seismic data show that the sills occur as oblique sheets or stepped transgressive sills towards the basin margins. When these oblique reflectors are extrapolated towards their origin in the SW, they appear to originate from a linear feeder zone in the centre of the basin (Fig. 4). This area is where the underlying crust has been stretched the most, and also where a lower-crustal high-velocity body both terminates and impinges on this thinned crust (Fig 1B). These critical observation lead us to interpret that the sills were fed from this lower-crustal-high velocity body, and that the magma moved from the zone of melting in the mantle, through highly stretched crystalline crust, and entered the basin along a linear north-south-oriented feeder-zone.

For the N Sill-complex, fewer seismic lines cross the origin of the sills, and imaging is poorer at depth compared to other parts of the basin. The orientation and shape of the northern magma feeder zone can therefore not be determined in the present dataset.

A 3D view of interpreted sills (Fig. 7) shows that the sills occur as two main shapes: The first type is sets of nested bowls sourced from either of the two distinct magma feeders in the northern and

southern parts of the basin. These sills have flat centres and show gradual transgression upwards through the basin towards the basin margins. These nested bowls can be up to 15 km deep and have a radius of 60 km, making them among the largest sills described globally (c.f. Wrona et al 2019). The second type of sills are flatter, up to 50 km long, follow stratigraphy to a greater degree, but also often transgress upwards towards the closest basin margins, and commonly occur in the centre of the basin and in the shallower parts (upper 4 km) of the basin (Fig. 6). This indicates that the sills follow the same stratigraphic intervals for great distances in the centre of the basin and towards the upper few kilometres in the basin, and that the sill segments that are deep and/or occur towards the margins of the basin have a greater tendency to transgress upwards through stratigraphy. This agrees with the upwards-towards-the-north stepping observed in the outcrop (Fig. 3A). Towards the SE margin of the study area, sills show a tendency to maintain their oblique trajectory even when intruding through tilted post-rift sediments and even basement. This important observation will be discussed below.

5.3 Dyke architecture in surface datasets

A large number of dykes have been mapped in the mainly vegetation-free plateaus of the Jameson Land Basin (Noe-Nygaard, 1976; Pedersen et al 2013; Fig. 2). A small number of these dykes cross-cut the sills, and this population of cross-cutting dykes is clearly younger than the sills and are believed to have been emplaced during the Oligocene plate-tectonic reorganization in the N Atlantic (Hald & Tegner, 2000). However, the vast majority of observed dykes are interconnected with, and geochemically similar to, the sills and believed to be emplaced at the same time as the sills (Hald & Tegner, 2000; Eide et al 2017). The dykes are 1-10 m wide, and the median width is 2.3 m (see DR2 for more statistics). More dykes are observed in the virtual outcrop where the exposure is excellent (Fig. 3A), than on the plateau (Fig 2). Many of the larger dykes observed in the virtual outcrop can be followed onto the plateau for several kilometres (Fig. 3H), showing that the dykes observed in the outcrop correspond to dykes mapped in the terrain.

From analysis of the virtual outcrop data, about 10% of the outcrop consists of intrusive rocks. Out of the intrusive material, 1% consists of dykes and 99% of sills (by area of outcrop on Fig. 3A, Eide et al 2017, see also DR2). The dykes in the study area are consistently oriented E-W to ESE-WNW, and no observed dykes in the Jameson Land Basin are oriented in the N-S direction (Fig 2B). This indicates that the magma pressure was great enough to form both sills and dykes at the same time, and that the EW compressive stress was greater than the NS compressive stress, which was then greater than the vertical compressive stress.

The dykes are most common in an area towards the south of the study area, and we term this the S Dyke Swarm (Fig. 2A). An area with elevated dyke density also occurs in the northern part of the Basin, and we term this the N Dyke Swarm (Fig. 2A). The S Dyke Swarm occurs at the eastern edge of the Lower Crustal High Velocity body (Fig 1B; Fig 2), and appears to radiate away from the origin of the S Sill-complex in the basin (i.e. as the mapped dykes are extrapolated towards the west, they intersect the interpreted origin of the S Sill-complex). The dykes in the N Dyke Swarm have a similar E-W to ESE-WNW orientation to the S Dyke Swarm, and it occurs in the middle between the S and N Sill-complexes, without any clear relation to any mapped geological feature.

5.4 Relationship between sill-complexes and dyke swarms in the Jameson Land Basin

Vertical and steeply dipping features such as dykes are difficult to image in reflection seismic data (e.g. Lecomte et al 2016), and their presence in the subsurface may be under-represented. However, dykes can in some instances be observed in seismic data nonetheless because they may (1) create discontinuities in otherwise tabular layers, (2) may have irregularities and thin associated sill intrusions that can be imaged, or (3) because they deform the host-rock in ways that can be imaged (e.g. Wall et al 2010; Minakov et al 2018; Eide et al 2018; Magee and Jackson, 2019). Because dykes in the Jameson Land Basin have been well-mapped throughout the available outcrop data (Fig. 2, Fig. 3H), it is possible to investigate their expression in seismic data by carefully studying the seismic data beneath and away from zones where dykes are mapped.

In seismic lines crossing the S Dyke Swarm, areas with several mapped dykes correspond to subvertical zones in the seismic data with a larger amount of noise and lower degree of reflector continuity (Fig 9a). We interpret that the poor imaging in these zones is related to the presence of dykes in these locations, and can assume a degree of understanding of the dyke distribution and architecture using the surface examples as a guide. These subvertical disturbance-zones appear to originate at the edge of dipping intrusive sheets (1 in Fig 8a) and the edges of relatively flat-lying sills (2 in Fig 8a). Thus, it appears that the S dyke swarm is fed from transgressive segments from large sills at great depth (10-15 km) in the basin. This again also implies that sills have a very important role in magma transport in the crust (Cartwright & Hansen, 2006; Muirhead et al 2014; Schofield et al 2015).

In seismic data from the N Sill Complex (Fig. 8b), no clear subvertical zones of disturbance can be observed in the areas where dykes are mapped, and the imaging is also poorer at depth (> 3 S TWT) in general, which may preclude observations of dykes. No correspondence between dykes and sills can therefore be demonstrated in this part of the basin.

5.5 Vertical connectivity of sills

The sills observed in the outcrop along Scoresby Sund (Fig. 3A) are locally transgressive, and do not show cross-cutting relationships but are rather interconnected with each other (Eide et al 2017). In the subsurface, sills are also transgressive, strongly interconnected, and appear to originate mainly from other sills and from short transgressive segments (steep oblique sheets, dykes) from underlying sills (Fig 9). This shows that significant magma transport through the crust can occur through interconnected sill networks rather than through dykes or dyke swarms alone. Although dykes may be underestimated in the subsurface seismic data, the low proportion of dykes compared to sills in the outcrop dataset offers an indication that dykes are in fact much less dominant in the basin than sills.

5.6 Thickness of sills

The sills in the studied outcrops along Hurry Inlet are 1-10 m thick (Fig 3a; Eide et al 2017). Geochemically similar sills up to 50 m thick have been reported from Ørsted Dal in the northern part of the basin (Hald & Tegner, 2000; Fig 2). In the seismic data, the vast majority of interpreted sills are reflections that are "tuned" (e.g. Widess, 1973), meaning they come from high impedance bodies that are so thin that reflections from top and bottom interfere with each other and their thickness cannot be determined (e.g. Fig. 9c). The tuning thickness varies from c. 25 m just below the present day surface to 80 m at 6 S TWT (c. 15 km), using velocities from Mandler & Jokat (1998) and frequencies measured from the reflection seismic dataset. This means that most of the sills are thinner than 25 m in the upper part of the basin, and thinner than 80 m in the deepest mart of the basin.

A small number of interpreted intrusions show a positive amplitude on top and a negative reflection at the base, and the thickest of these has an apparent thickness of 30 ms, which would correspond to a thickness of 100 m (Fig. 9a). However, based on the complex geometries of these reflections, it is possible that these reflections represent several closely spaced thinner intrusions rather than one single 100 m thick intrusion (see Eide et al 2018). Sills throughout the NAIP commonly range in thickness from 10 to c. 100 m thick (e.g. Hansen et al., 2011; Schofiled et al., 2016; Fyfe et al., 2021). Known sill thickness within other large igneous provinces can be up to c 300 m thick (e.g. Jerram et al., 2010; Svensen et al., 2018), and this was earlier believed to also be the case within the deeper parts of Jameson Land (Larsen & Marcussen et al 1992). However, within the current dataset we have not seen evidence of sills as thick as 300 m, as interpreted earlier by Larsen & Marcussen et al (1992). This highlights the importance of data quality in subsurface estimation of sill thicknesses (Planke et al., 2015).

6. Discussion

6.1 Magma transport through the crust and sedimentary basins

Based on the observations made from the Jameson Land Basin in East Greenland, we present a model for magma transport from the mantle, through the thinned crystalline crust and through the Jameson Land Basin (Fig. 10). We suggest that this model is relevant for understanding transport of magma from the mantle to the surface also in other parts of the world where predominantly mafic magma is emplaced into thick sedimentary basins, and that transport of mafic magma through sedimentary basins is distinctively different from magmatism that transits through crystalline crust. This is mainly due to the low viscosity of basaltic magma, the weak and stratified nature of sedimentary host rocks (see section 6.3), and of the progressive changes in mechanical properties of sedimentary host-rock with depth.

6.1.1 Transport of magma into sedimentary basin

Seismic refraction data from the Jameson Land has identified the presence of a lower crustal high velocity body at the base of the crust c 20 km below the present-day surface of the Jameson Land Basin (Fig. 1B, Weigel et al 1995; Mandler & Jokat 1998). This body is inclined and its highest point lies directly beneath the base of the Jameson Land Basin, where the continental crust is highly thinned. The seismic data images sills down to the base of the sedimentary basin c. 15 km below the present-day surface, and the architecture of sills in the S of the basin show they are supplied from a N-S-trending zone in the centre of the basin (Figs 4, 7). This strongly suggests that the mafic intrusives in the basin were supplied from magma chambers below the crust represented by the lower-crustal high-velocity body (Fig 10). This lower-crustal body and other examples of such high-velocity bodies along the East Greenland margin and on the conjugate mid-Norway Margin, are interpreted to result from voluminous magmatic underplating (e.g. Voss & Jokat 2007, Neumann et al 2013). Such magmatic underplating is commonly thought to result from the addition of mafic magma to the lower crust and uppermost mantle around the Moho (see Thybo & Artemieva, 2013), and is likely to include the development of extensive magma bodies, where fractionation processes can result in more evolved magmas than the primary high-temperature mantle melts. The evolved basaltic melts we find in the Jameson Land Basin (with 5-7 weight percent MgO; Hald & Tegner

2000), are likely to be the result of such underplating processes (e.g. Cox, 1993), with the resulting melts transiting the crust where the crystalline basement is thinnest and weakest. The architecture of intrusives in the area where the sills transit through the crystalline crust is not constrained by seismic data, but the narrowness of the magmatic feeder-zone and the lack of any perceptible offset between the feeder zone and the top of the magmatic underplate, suggests that magma transport through the crystalline crust must have been through localized, near-vertical dykes along the basin axis (Fig. 10B). As magma transport through the sill-dominated intrusive network in the sedimentary basin is much more distributed than through this narrow zone in the crystalline crust, magma supply through this zone must have been very large per unit volume compared to in the sedimentary basin.

6.1.2 Sills and volcanoes significantly offset from magma sources and main feeder zones

The deeper sills fed from the magma feeder zone and emplaced in the lower parts of the Jameson Land Basin are bowl-shaped and radiate outwards and upwards away from the feeder zone (Figs. 4, 7). Sills observed in outcrops today originated from magmas fed from at least 50 km away (Fig. 2), and this implies that the majority of sills and possibly volcanoes in similar settings may be offset by many tens of kilometres away from where the magma was generated in the upper mantle and injected into the basin (Fig. 10). This supports earlier work on lateral magma-transport in sedimentary basins (e.g. Magee et al 2016). The seismic data presented here clearly shows two geographically distinct magma feeder zones for the southern and northern sill-complexes (Fig. 7). Although the geochemistry of igneous intrusives in the Jameson Land Basin has been studied (Hald & Tegner, 2000), there is no evidence yet of distinct geochemical signatures of magma that correspond to these two feeder zones identified in the seismic data. Investigating geochemical and geochronological data from this area with the aim to characterize these two complexes would be highly interesting, particularly to see if they come from a similar or different source region.

6.1.3 Lack of magma chambers and volcanic centres within the basin

Geophysical and geochemical data show that many large modern volcanoes are underlain by complex zones of low seismic velocities that are interpreted as magma chambers (e.g. Jaxybulatov et al 2014, Huang et al 2015). Such magma chambers could be analogous to plutons and laccoliths in

ancient systems, but plutons and laccoliths appear to be more common in silicic and andesitic systems (Jerram and Bryan, 2015). Although mafic laccoliths and other large-scale intrusive mafic bodies occur in sedimentary basins and upper crust (e.g Jackson and Pollard 1988; Monreal et al 2009; Holness et al, 2017; Walker et el., 2021), they are smaller and less common in volume and extent compared to sills in large sedimentary basins studied in large outcrops and extensive seismic datasets (e.g. Eide et al 2016; Polteau et al 2016; Schofield et al 2017; Coetzee & Kisters, 2017; Reynolds et al., 2017; Svensen et al 2018; Gilmullina et al 2021). For example, the volcanic centre of Rum in Scotland is approximately 200 km^2 in extent, while it's associated Little Minch Sill-complex covers an area 20 times larger (c. 4 000 km^2, Fyfe et al 2021).

Volcanic centres associated with large igneous provinces can be quite large, and are commonly characterised by multiple pulsed magmatic events and transitions from mafic through to silicic compositions (Jerram and Bryan, 2015). In some offshore sequences along volcanic rifted margins such complexes are recognised through complex seismic zones, often with significant gravity and magnetic anomalies, and highlight the location of candidate volcanic centres within the magmatic plumbing systems (e.g. Emeleus and Bell, 2005, Kilhams et al., 2021, Walker et al., 2021). Many large, isolated centres are known within the North Atlantic Igneous Province (NAIP) along the British Paleaogene sections (e.g. Emeleus and Bell, 2005; Schofield et al. 2017), and some centres have also been realised recently along the Norwegian Margin (e.g. Kilhams et al., 2021). Many of these volcanic centres are known to be associated with long-lived, pre-existing, crustal-scale faults and lineaments (e.g Fyfe et al 2021). In Central East Greenland, there are also several large igneous centres, such as the Werner Bjerge Complex at the NW margin of the Jameson Land Basin (Fig. 2A), but these are also associated with magma intrusion along basin margins and crustal-scale faults, and these are associated with younger and more felsic magmas (Brooks et al 2010).

In contrast, the Jameson Land Basin itself is dominated by sills that are tens of kilometres long and wide, and (likely much) less than 80 m thick. No candidates for large-scale magma chambers are observed within the Jameson Land Basin. Further along this same margin, the Danmarkshavn and Tethis basins within offshore East Greenland, also show extensive sill complexes with, as yet, no

clear igneous centres identified (Reynolds et al., 2017). This, combined with observations from other sedimentary basins described above, suggests that such large-scale crustal mafic magma chambers are somewhat limited compared to sill complexes within thick sedimentary sequences, *and* that there are large-scale geological controls on the development of sill-complexes versus localized igneous centres: mafic magmas are likely to create distributed sill-complexes *within* sedimentary basins due to the low viscosity of basaltic magma (e.g. Shaw et al 1968, Wada, 1994), and the weak and layered nature of host-rocks. Large-scale subsurface mafic magma chambers may be more likely to form when large amounts of magma are supplied along structural and possibly major lithological discontinuities. If such magma chambers are present *at the bases* of sedimentary basins near structural entry-points through the underlying crystalline crust (such as the feeder-zone below the Jameson Land Basin, Fig. 10), it would indeed be difficult to detect them in seismic data as these would be located under thick sedimentary piles and close to basement rocks with little seismic impedance contrast.

Using simple assumptions for the shape of the Southern Sill Complexes and the individual sills within it (the sill-complex is symmetrical across the N-S axis, the sill-complex can be approximated as a cone, the proportion of sills at depth are comparable to what is observed in the outcrop dataset in Fig. 3A), we calculate the volume of magma in the S sill-complex to be between 110 to 5600 km^3 (see DR3 for details). This large uncertainty is due to the uncertainty in estimating thickness of sills at depth. This calculated magma volume in the Southern Sill-complex is 4 to 20 times the volume of the well-known Skaergaard Intrusion (Nielsen 2004). This shows that the volume of sill-complexes can be significant and that in sedimentary basins.

6.2 Relation of studied igneous intrusions to regional tectonics

Palaeogene dykes are widespread across most of the Jameson Land Basin (Fig. 2A), and occur as two separate dyke swarms, one in the north and one in south of the basin (Fig. 2A). The dykes are oriented E-W to ENE-WSW, and no dykes occur in the N-S direction (Fig 2B). In outcrop data, 100 times more magma has been emplaced as sills compared to dykes (by area of outcrop), and the

vertical extension by sills is 100 greater than the lateral extension by dykes (Fig. 3A). Based on the large amounts of sills imaged in seismic data at all basin depths, we assume that these relationships also hold throughout the basin. This implies that the stress-state at time of emplacement had the axis of least compressive stress (σ_3) oriented vertically (to allow for a large amount of sills to be emplaced), intermediate compressive stress (σ_2) oriented N-S (to allow for a smaller amount of dykes to open in the E-W direction), maximum compressive stress (σ_1) oriented E-W (to prevent N-S dykes from opening), and magma pressure comparable to σ_2 (to account for the smaller amounts of intrusives in E-W dykes).

It is likely that the interpreted E-W-oriented maximum compressive stress at time of emplacement was due to ridge-push from the Ægir spreading rigde in the Norwegian Sea, which started spreading at c. 55 Ma (Fig. 10A; e.g. Blischke et al 2017), 2 Myr before the age of emplacement for the Jameson Land Intrusives (Hald & Tegner, 2000). The 53 Ma igneous complex has been interpreted by Hald and Tegner (2000) to represent rifting associated with a failed attempt at a westwards ridge jump, similar to the ridge jump that occurred during the late Eocene–Oligocene and rifted off the Jan Mayen microcontinent (Talwani & Eldholm 1977; Mjelde et al 2008; Gaina et al 2009). However, the dyke orientations in Jameson Land are not consistent with rifting in the east-west direction. The exact mechanism that led to the emplacement of the sill-complexes in Jameson Land is therefore unclear. Only one sill and one dyke have been dated hitherto using Ar-Ar and palaeomagnetism (Hald and Tegner 2000), and clearly a more robust and comprehensive age data set (ideally with more precise U-Pb dates if possible) would be beneficial to improve the understanding of this intrusive complex and its relation to the regional tectonics.

The great distance (c. 150 km) between the magmatic underplate below Jameson Land and the continent-ocean transition at time of breakup is unusual (Voss and Jokat, 2007; Voss et al 2009). The crustal thinning below the Jameson Land Basin was mainly set up through post-Caledonian to Triassic extension (Fig. 10A), and this likely led to weakening of the crust that led to the capture of

magma in the Jameson Land Basin. This is thus an example of deep-seated basin structure influencing magma input a long time after the crustal structure was made.

6.3 Why do sills follow mudstones?

Sills observed in the outcrop dataset from Jameson Land are preferentially emplaced within, and propagated along, mudstones (Fig. 3). Similar trends are also seen in other areas (e.g. Parsons et al 2017; Spacapan et al 2017; Mark et al 2018), and here we offer an explanation of why this happens:

Brittle host-rocks in contact with an inflating magma-filled conduit will rupture and an intrusion will propagate, when the following condition is satisfied (Gudmundsson, 1990):

$$p_l + p_e = \sigma_3 + T_0 \qquad \text{(eq. 1)}$$

where p_l is the lithostatic pressure, p_e is the magma overpressure with regards to lithostatic pressure at time of failure, σ_3 is the least compressive stress or maximum tensile stress, and T_0 is the in situ tensile strength at the failure location. The stress-state is often discussed in studies of igneous intrusions (e.g. Barnett & Gudmundsson 2014), while the tensile strength of host-rock has commonly received much less attention. Tensile stress is often regarded as a property that varies relatively little (0.5 - 6 MPa), perhaps because these models were originally developed for basaltic lava piles (Gudmundson 1990; 2006).

In sedimentary basins, lithologies are variable and mudstones are common both as thick (meters to kilometers thick layers, and mm-to-cm-scale drapes (Fig 3). Clay-rich mudstones, and in particular mudstones with a well-developed fissility *("shales")*, split easily along bedding planes (Fig. 11). The tensile strength (in MPa) of mudstones has been measured to be c. 300 times lower parallel to the bedding plane compared to perpendicular to the bedding plane (Gao et al 2015). Many mudstones thus have a strong tensile stress anisotropy oriented along the bedding planes. It follows from Equation 1 that if tensile strength is small enough, fractures can develop in directions that are not parallel to σ_3. A high tensile stress anisotropy can explain why mudstones are so easily intruded, and why nearly all dyke-to-sill-transitions in the Hurry Inlet outcrop occur within mudstones (Fig. 3A, Eide et al 2017). It is also worth noting that σ_3 does not have to be determined by far-field tectonic

stress alone, but can be local as significant local stresses occur in and around propagating sill-complexes (e.g. Schofield et al 2012; Poppe et al 2000).

6.4 Controls on overall transgressive sill architecture

6.4.1 Description of overall sill architecture

On the scale of kilometres, sills mapped in the Hurry Inlet outcrop show a prominent upwards-towards-the-north stepping through the stratigraphy at an angle of c 6° (green arrows in Fig. 3A). A similar upwards-towards-basin-margins stepping of sills is observed deep in the basin in seismic data (orange arrows in Figs. 4, 5, 7). In most of the basin, particular in the basin centre and in the upper post-rift deposits, the sills are strongly concordant to host-rock layering. In other places, particularly towards basin margins, oblique intrusive sheets cross-cut flat-lying bedding, tilted syn-rift bedding and even crystalline basement without changing their attitude (Fig. 5A).

Although sills often appear as oblique sheets in the seismic data, it is likely that many of the sills at depth are in fact stepped and segmented rather than truly oblique (compare Fig. 3B,C), as no oblique sheets are observed in the outcrops. The transgressive segments of the sills in the outcrop dataset (Fig. 3A) are not controlled by any apparent host-rock features such as faults, fractures, or discontinuous sedimentary bodies. The host-rock in the outcrop is laterally homogeneous apart from a gradual increase in sandstone content towards the north, and it is generally un-faulted and has few fractures (Eide et al 2016). We therefore believe the organized nature of transgressive sill segments and upwards stepping of sills, from injection centres in the deep basin towards the surface at basin margins, is mainly controlled by stresses in the basin interacting with the host-rock and local stresses from the propagating sill intrusions.

6.4.2 Controls on meter-to-kilometre-scale sill architecture

The lateral variation in lithology in the outcrop (Fig. 3A) allows us to investigate how changing host-rock properties influence architecture of sills. The proportion of sandstone decreases towards the south in the sand-rich stratigraphic units (Fig. 3A; Eide et al 2016;), leading to a high-contrast succession in the north, with layers with strong difference in sandstone content, and a low-contrast succession in the southern part of the outcrop, where there is little difference in sand-content in the

stratigraphy (Fig. 12). In the S parts of the outcrop, with mud-rich deposits throughout, sills consist of c 200 m wide segments which gradually transgress upwards and are linked by vertical jogs 1-10 m high (Fig 12). In the middle of the outcrop, with intermediate sandstone content, sills segments are c. 1 km long and separated by c. 25-35 m upward-to-the-north jogs. In the high-contrast part in the north, sills follow mudstone intervals for much longer distances, up to 6 km, and transgress out of the sand-rich intervals over short distances. Sill segments here are joined by a single, c 150 m high jog.

The observations above have a set of important implications (Figs 12; 13): (1) On the outcrop-scale (< 200 m), the intrusions in the Jameson Land predominantly follow bed boundaries and especially mudstones (Fig 3). This implies strong host-rock control on sill architecture. Any sill transgressions observed in smaller outcrops (less than a few hundred meters) could easily be interpreted to be random, and large-scale stress-related controls on sill intrusions are likely to be underestimated from such smaller outcrops. (2) On the large-scale (> 5 km), sills rather follow trajectories concordant with the overall structure of the sills in the basin – upwards-towards the basin-margins (Fig. 13). This implies that regional stress field has a strong control on sill intrusions at larger scales (Walker et al 2017; Stephens et al 2017; Walker & Gill, 2020), that the stress-controls are largest towards the basin margins, and that stress-controls diminishes towards the basin centre. It is possible that the basin fill is more sandstone rich near the basin margins, because of proximity to the clastic sediment source (Fig. 13). This further promotes stress-related controls on intrusion architecture near basin margins as weak mudstones are rarer close to basin margins due to increased sand supply. (3) On intermediate scales (0.5-5 km), the controls on sill architecture are more variable. In areas of low host-rock contrast, sills consist of c. 200 m long segments and show regular steps upwards through stratigraphy, leading to a stepped oblique sill which goes upwards at c. 6°. In areas of high host-rock-contrast, sills occur in regional mudstones and transgress, but the segment lengths and step heights are much greater (6 km, 150 m; Fig. 12).

6.4.3 Depth control on large-scale sill morphology

On even larger scales, sill geometries in the Jameson Land Basin change with depth. From the surface down to c. 10 km depth in the Jameson Land Basin, sills appear to be mainly layer-concordant or obliquely transgressive, and appear to have been emplaced and accommodated mainly by brittle processes. This present-day depth interval corresponds to depths of 3-13 km at time of emplacement. In brittle, cemented host rocks, the lithological controls on sill emplacement are strong, and sills generally follow weak layers in host-rock stratigraphy instead of developing saucer-shapes (e.g. Schofield et al 2012; Eide et al 2017), which are common in uncemented, shallowly buried sediments (Fig. 13).

In the deep (>10 km) parts of the basin (corresponding to depths of more than 13 km at time of emplacement) the sills form large bowl-shaped geometries (Figs. 6, 7). These bowl-shapes are similar to shallow saucers, but they have much larger diameters: a few tens of m for shallow saucers (Polteau et al 2008) versus up to 50 km for the deep sills in the Jameson Land Basin. The brittle/ductile transition zone generally occurs around a temperature of about 300°C (e.g. Aharonov and Scholz, 2019). Using a paleo-geothermal gradient in the Jameson Land Basin of 30°C/km (Green and Japsen, 2018), the brittle-ductile transition would have been at c 10 km depth at time of emplacement of the sills, which fits well with the observed gross changes in sill geometries with depth (Fig. 13). It is therefore likely that the large bowl-shaped geometries are related to a change in emplacement mechanism of magma within partly ductile rocks. Polteau et al (2008) showed that diameter of saucer-shaped sills increases with depth, something that fits well with the very large diameter of the deep seated sills in the Jameson Land. Thus, it seems that saucer-shaped sills are common in host-rocks that may behave in a non-brittle manner (ductile rocks and uncemented sediments), but that development of saucer-shaped sills is inhibited in the depth interval where clastic sediments are commonly cemented and brittle from c. 2.5-10 km depth. Different emplacement mechanisms and architectures below the brittle-ductile transition zone has been reported before from igneous dykes (Kjøll et al 2019).

7. Conclusions

The Jameson Land basin is a unique place to study the evolution of mafic sill-complexes on the basin scale because of the combination of c 3 km of erosion that expose intrusive elements in excellent exposures, deep reflection-seismic lines, and abundant previous studies on stratigraphy, geochemistry and crustal structure. These are our main findings from investigating these datasets together:

1. At least one of the two sills complexes in the Jameson Land Basin is fed from where a lower-crustal high-velocity body impinges on highly stretched crystalline crust below the basin.
2. Sills propagate upwards and outwards into the basin, away from linear magma feeder zones at the base of the basin. Sill-complexes are shaped as nested bowls that have a maximum radius of c 60 km and depth of 15 km.
3. On scales from 0.2-6 km, the architecture of sill-complexes are strongly controlled by host-rock lithology, and sills generally follow the sedimentary layering. On scales from centimetres to 0.2 km, sill architecture is mainly determined by weak mudstone beds which the sills follow. The sills follow mudstones because of the strong tensile strength anisotropy of mudstone, which makes it possible to open fractures in mudstones regardless of the tectonic stress state.
4. Sills are generally layer-concordant in the basin centre and transgress obliquely towards basin margins. The main reason for this is likely the distribution of stresses in the basin and higher sandstone-content near basin-margin that yields fewer weak mudstone beds to intrude into.
5. Sills that are emplaced below the brittle-ductile transition zone, show a change in geometry to larger bowl-shaped morphologies.

6. Any magma chambers in the form of laccoliths or stocks are not observed in the Jameson Land Basin. It appears likely that magma transport mainly through interconnected sills is common for mafic systems within sedimentary basins, while large intrusive magmatic bodies are associated with crustal scale faults through crystalline rocks.
7. The orientation WNW-ESE orientation of igneous dykes makes us doubt the existing geodynamic interpretations for the origin of the studied sills in the Jameson Land, where they were emplaced because of EW-directed rifting associated with a failed, early attempt of a westwards ridge jump in the area.

In summary, these observations and ideas highlight that mafic igneous systems that intrude thick sedimentary basins are different from traditional models of magma transport through the crust. In particular, the Jameson Land Basin is characterized by a lack of crustal magma chambers, magma transport largely through interconnected sills, and strong host-rock *and* strong stress-related controls on sill-complex architecture. Furthermore, this study shows that there is great potential to generate further understanding of basin-scale magma transport through integrated, targeted geochemical and geochronological studies of this well-exposed sill-complex.

8. Acknowledgements:

We thank reviewers Sam Poppe, Janine Kavanagh and Christian Tegner for thorough reviews that significantly improved this paper. Funding for data acquisition was provided from the Research Council of Norway through the PETROMAKS project 193059 and the FORCE Safari project. Funding for data analysis provided from PETROMAKS through the ISBAR project 267689. Dougal Jerram is partly funded through the Research Council of Norway through its Centre of Excellence funding scheme, project number 223272, CEED. We acknowledge Geological Survey of Denmark and Greenland (GEUS) for access to, and permission to publish images of, onshore seismic data acquired by Atlantic Richfield Company (ARCO). Schlumberger are acknowledged for an academic license for Petrel which was used for seismic interpretation and visualization. Gijs Henstra, Bjørn Nyberg and Simon Buckley are thanked for assistance with fieldwork and data processing. The virtual outcrop was visualized and interpreted using LIME (http://virtualoutcrop.com/lime; Buckley et al 2019). The outcrop dataset at Hurry Inlet is available from the VOG group at https://v3geo.com/model/61.

9. Captions

Fig 1: A) Topography and bathymetry of the North Atlantic, and features mentioned in the paper. The study area is conjugate to the Møre Margin offshore Western Norway. B) Cross-section showing the crustal structure in and around the study area (from Weigel et al. 1995), and igneous sills mapped as part of this study. Note that the sills occur above where a lower crustal high-velocity body (magmatic underplate) impinges on the crust at the base of the deep Jameson Land Basin. C) P-wave velocities measured from refraction seismic data in the Jameson Land basin (Mandler & Jokat et al 1998), compared to seismic velocities in deep wells on the Norwegian Continental Shelf, see A for location. *[Dimensions: Full page width]*

Fig. 2: A) Geological map of the study area in Jameson Land, modified from the seamless digital 1:500 000 scale geological map of Greenland (Pedersen et al 2013). Note the generally flat and un-faulted nature of the post-rift sediments, and the presence of large amounts of WNW-ESE dykes. Lines with black, dashed black, dashed green, yellow, and dashed red color show location of seismic cross-sections shown in later figures. B) Orientation of dykes in the geological map of Jameson Land Basin. C) Simplified map showing distribution of interpreted sill-complexes, magma entry points to the basin, and dyke swarms within the basin, and the location of the lower-crustal body. *[Dimensions: Full page]*

Fig. 3: Key observations of igneous intrusions in virtual outcrop data from the outcrop along Hurry Inlet. For location, see Fig. 2A. A) Overview of sill architecture. White outlines show extent of outcrop, interpretations outside outlines are extrapolated. Black boxes show location of later subfigures D-H. Note the large proportion of sills compared to dykes (c. 99% sills by outcrop area), the overall upwards-towards-the-north stepping of sills (green dashed lines), obvious feeding relationships between dykes and sills, the tendency for sills to transgress stepwise upwards towards

the north in the southern part, and to follow extensive mudstones in the northern part, and turn from sills to dykes without any changes in the host-rock (pinchout of sedimentary bodies, faults). B) Synthetic seismogram (from Eide et al 2018) showing what (A) would look like in seismic data at c. 6 km depth. Note that dykes are not detected, that reflections from several sills interfere and appear as one, and that actually stepped sills appear oblique sheets. C) Synthetic seismogram (from Eide et al 2018) showing what (A) would look like in seismic data at c. 3 km depth. Note that dykes are in some cases possible to detect, and that geometries of sills c.10 m thick are well-constrained at these shallower depths. D) Feeding-relationships between dykes and sills, and that sills step upwards-towards-the-north through the stratigraphy. E) Abrupt transition from sill to dyke without any clear structural or lithological cause. F) Image showing one vertically stable sill emplaced in a regional mudstone bed, and one less stable sill emplaced in poorly cemented sand. G) Thin sills that seek out very small mudstone-drapes in crossbed foresets to intrude into, indicating very strong host-rock controls on sill emplacement. H) 3D composite image of virtual outcrop and Google Earth imagery (Image © Maxar Technologies) showing that dykes can be observed both in vertical outcrops and the nearly vegetation-free plateaus in Jameson Land, making them easy to map over large areas. *[Dimensions: Full page]*

Fig. 4: Large-scale 3D view at depth showing the geometry of the Jameson Land Basin, basin fill and igneous intrusions. Note that the sills show nested bowl-shapes at depth and propagate obliquely upwards, broadly concordant with the overall basin shape, and that the sills become flatter in the upper parts of the basin fill. Also note that the bowl-shaped sills appear to be fed from a magma entry zone along the centre of the basin, and that steep-southern sills appear to be supplied from an out-of plane magma feeder zone. The magma entry zone broadly coincides with where the lower crustal body impinges on the base of the Jameson Land Basin (Figs 1B, 2A). Inset labelled "amplitude" shows color scale for seismic data. For location, see Fig 2. For un-interpreted and un-warped versions of the seismic data, see DR1. *[Dimensions: Full page width]*

Fig. 5: 3D view of the Jameson Land Basin, showing relationships between bedding architecture, lithology and igneous intrusions at depth. Note angle of sills is relatively constant at depth, and that

sills cross-cut basement (1) and bedding in pre-rift (2) and syn-rift (3). In some areas, sills follow the trends of nearby faults (4), likely indicating that some minor faults parallel to the major faults were exploited by sills for short distances. Sills in the post-rift and the syn-rift in the basin centre (5) are generally concordant with layering, but transgress upwards towards the basin margins. Inset labelled "amplitude" shows color scale for seismic data, and shows how are be interpreted from seismic data. B) Un-interpreted and un-warped view of the seismic line on the S face of the illustration in A. C) 1D seismic response from a tuned (thin) high impedance reflector. *[Dimensions: Full page width]*

Fig. 6: A) Composite 2D seismic line showing the two sill-complexes and their sources in the south and north of the basin. Note that two major dyke swarms are offset from the magma feeder zone of the sill-complexes. B) Interpreted version of A. C) Simplified map of study area showing orientation of seismic line in relation to important features discussed in the paper. *[Dimensions: Rotated full page]*

Fig. 7: A) 3D view of mapped sills in the Jameson Land Basin. Note that the sills occur as nested bowls sourced from two distinct areas, the southern source and the northern source. Also note that a zone exists where the sills from the N and the S sill-complexes overlap, and that this zone coincides with the location of the N dyke swarm. B) Simplified map of study area showing orientation of seismic line in relation to important features discussed in the paper, and showing 3D view. *[Dimensions: Full page width]*

Fig. 8: Seismic 2D lines through the S (A) and N (B) dyke swarms and adjacent geological maps. Map legend is presented in Fig. 2. A) In the S dyke swarm, areas with several dykes correspond to near-vertical zones of more noise on the seismic images. These zones appear to have origins at the tips of (1) high- and (2) low-angle sills at great depths in the basin, indicating that dykes are mainly sourced from transgressive edges of sills deep in the basin. B) The seismic lines from the N dyke swarm show in general few vertical features that can be attributed to the dykes mapped in the surface, and no particular architecture of sills that can be related to the dykes. It is unclear whether this is real or if it is an effect of poorer data quality here. (C) Map showing location of seismic lines and dyke swarms. *[Dimensions: 1.5 coloumns? Full page width? – whatever convenient]*

Fig. 9: Typical 2D seismic line (interpreted in A, uninterpreted in B) in the Jameson Land Basin. Note (1) the considerable vertical connectivity of sills, indicating that dykes are not necessary to transport large amounts of magma through the crust, and (2) the absence of thick or outsized sills, indicating that magma transport was through a complicated sill network, and that any crustal magma chambers were absent. (C) Explanation of the tuning effect. See Fig. 2 for location. *[Dimensions: 1.5 coloumns? Full page width? – whatever convenient]*

Fig. 10: A) Tectonic setting of the Jameson Land Basin at time of emplacement of the 53 Ma intrusions (modified from Mjelde et al 2008). B) Compilation of key observations of the relationship between magmatic plumbing networks, their host-rocks and regional tectonics made in the Jameson Land study area. 1: Accumulation of residual melt from localized mantle melting. 2: Transit of magma through narrow zone of highly stretched crystalline crust above where mantle melting impinges on crust. 3: Formation of deep-seated intrusions that are flatter in the basin centre and transgress obliquely towards basin margins. 4: Magma transport in basin mainly through interconnected sills. A small proportion intrusive material occurs as dykes sourced from deep sills. 5-6: Sills in upper 5 km of basin mainly strata-concordant, but highly transgressive towards basin margins (6). Sills occasionally exploit faults. 7: Formation of relatively isolated dyke swarms close to magma sources and in areas where sill-complexes interact. *[Dimensions: Full page width]*

Fig. 11: Pictures of fissile shales (A: Middle Jurassic Ness Formation, Dunlin Field, North Sea, B: Jameson Land study area, C: Middle Jurassic Great Estuarine Group, Isle of Skye) illustrating the strong tendency for mudstone to develop layer-parallel parting planes (arrows). This leads to a pronounced tensile strength anisotropy of mudstones, with lower tensile strength normal to layering. Igneous sills are therefore, as in (C), often emplaced within and parallel to such mudstones. *[Dimensions: Full page width]*

Fig. 12: Conceptual diagram showing the interplay between regional stress field and host-rock heterogeneity on sill-complex architectures in areas where sill emplacement is also controlled by stress. In the left part, vertical host-rock heterogeneity is low and stepwise sills transgressions occur

at short (c. 200 m) intervals. In the right part, where vertical host-rock heterogeneity is high, sills make much greater (up to 3 km) deviations from the directions set up by the regional stress field. *[Dimensions: Full page width]*

Fig. 13: Conceptual model of mafic sill-complexes emplaced in thick sedimentary basins, showing expected geometries in the Jameson Land Basin at time of emplacement. Note the narrow magma feeder-zone below the middle of the basin, the change of intrusion architecture with depth and changing host-rock architecture, the upwards-towards-basin margins propagation of sills, and the offset between fissure volcanism and the magma feeder zone. *[Dimensions: Full page width]*

10. References

Ahokas, J.M., Nystuen, J.P. and Martinius, A.W., 2014. Depositional dynamics and sequence development in a tidally influenced marginal marine basin: Early Jurassic Neill Klinter Group, Jameson Land Basin, East Greenland. From Depositional Systems to Sedimentary Successions on the Norwegian Continental Margin. International Association of Sedimentologists Special Publications, 46, pp.291-338.

Aharonov, E., & Scholz, C. H. (2019). The brittle-ductile transition predicted by a physics-based friction law. Journal of Geophysical Research: Solid Earth,124, 2721–2737. https://doi.org/10.1029/2018JB016878

Barnett, Z.A. and Gudmundsson, A., 2014. Numerical modelling of dykes deflected into sills to form a magma chamber. Journal of Volcanology and Geothermal Research, 281, pp.1-11.

Bengaard H.J. and Henriksen, N., 1982. Geological Map of Greenland Sheet 12 Scoresby Sund. Geological Survey of Denmark and Greenland. Geodætisk Institut

Bjørlykke, K. and Egeberg, P.K., 1993. Quartz cementation in sedimentary basins. AAPG bulletin, 77(9), pp.1538-1548.

Blischke, A., Gaina, C., Hopper, J.R., Péron-Pinvidic, G., Brandsdóttir, B., Guarnieri, P., Erlendsson, Ö. and Gunnarsson, K., 2017. The Jan Mayen microcontinent: an update of its architecture, structural development and role during the transition from the Ægir Ridge to the mid-oceanic Kolbeinsey Ridge. Geological Society, London, Special Publications, 447(1), pp.299-337.

Brethes, A., Guarnieri, P., Rasmussen, T.M. and Bauer, T.E., 2018. Interpretation of aeromagnetic data in the Jameson Land Basin, central East Greenland: Structures and related mineralized systems. Tectonophysics, 724, pp.116-136.

Brooks, C.K. 2011. The East Greenland rifted volcanic margin. Geological Survey of Denmark and Greenland Bulletin, 24, 96.

Buckley, S.J., Howell, J.A., Enge, H.D. and Kurz, T.H., 2008. Terrestrial laser scanning in geology: data acquisition, processing and accuracy considerations. Journal of the Geological Society, 165(3), pp.625-638.

Buckley, S.J., Ringdal, K., Naumann, N., Dolva, B., Kurz, T.H., Howell, J.A. and Dewez, T.J., 2019. LIME: Software for 3-D visualization, interpretation, and communication of virtual geoscience models. Geosphere, 15(1), pp.222-235.

Cartwright, J. and Huuse, M., 2005. 3D seismic technology: the geological 'Hubble'. Basin Research, 17(1), pp.1-20.

Cartwright, J. and Møller Hansen, D., 2006. Magma transport through the crust via interconnected sill complexes. Geology, 34(11), pp.929-932.

Coetzee, A. and Kisters, A.F.M., 2017. Dyke-sill relationships in Karoo dolerites as indicators of propagation and emplacement processes of mafic magmas in the shallow crust. Journal of Structural Geology, 97, pp.172-188.

Costa, F., Shea, T. and Ubide, T., 2020. Diffusion chronometry and the timescales of magmatic processes. Nature Reviews Earth & Environment, 1(4), pp.201-214.

Cox, K.G., 1993. Continental magmatic underplating. Philosophical Transactions of the Royal Society of London. Series A: Physical and Engineering Sciences, 342(1663), pp.155-166.

Dam, G. and Surlyk, F., 1998. Stratigraphy of the Neill Klinter Group; a Lower–lower Middle Jurassic tidal embayment succession, Jameson land, east Greenland. Geology of Greenland Survey Bulletin, 175, pp.1-80.

Eide, C.H., Howell, J.A., Buckley, S.J., Martinius, A.W., Oftedal, B.T. and Henstra, G.A., 2016. Facies model for a coarse-grained, tide-influenced delta: Gule Horn Formation (early Jurassic), Jameson Land, Greenland. Sedimentology, 63(6), pp.1474-1506.

Eide, C.H., Klausen, T.G., Katkov, D., Suslova, A.A. and Helland-Hansen, W., 2018. Linking an Early Triassic delta to antecedent topography: Source-to-sink study of the southwestern Barents Sea margin. Bulletin, 130(1-2), pp.263-283.

Eide, C.H., Schofield, N., Jerram, D.A. and Howell, J.A., 2017. Basin-scale architecture of deeply emplaced sill complexes: Jameson Land, East Greenland. Journal of the Geological Society, 174(1), pp.23-40.

Eide, C.H., Schofield, N., Lecomte, I., Buckley, S.J. and Howell, J.A., 2018. Seismic interpretation of sill complexes in sedimentary basins: implications for the sub-sill imaging problem. Journal of the Geological Society, 175(2), pp.193-209.

Elders, W.A., Friðleifsson, G.Ó. and Albertsson, A., 2014. Drilling into magma and the implications of the Iceland Deep Drilling Project (IDDP) for high-temperature geothermal systems worldwide. Geothermics, 49, pp.111-118.

Emeleus, C H, and Bell, B R. 2005. British regional geology: The Palaeogene volcanic districts of Scotland. Fourth edition. Keyworth, Nottingham: British Geological Survey, pp 214.

Fyfe, L-J. C., Schofield, N., Holford, S. P., Jerram, D. A., Hartley, A., 2021. Emplacement of the Little Minch Sill Complex, Sea of Hebrides Basin, NW Scotland. Journal of the Geological Society 2021; doi: https://doi.org/10.1144/jgs2020-177

Gaina, C., Gernigon, L. and Ball, P., 2009. Palaeocene–Recent plate boundaries in the NE Atlantic and the formation of the Jan Mayen microcontinent. Journal of the Geological Society, 166(4), pp.601-616.

Galland, O., 2012. Experimental modelling of ground deformation associated with shallow magma intrusions. Earth and Planetary Science Letters, 317, pp.145-156.

Gao, Q., Tao, J., Hu, J. and Yu, X.B., 2015. Laboratory study on the mechanical behaviors of an anisotropic shale rock. Journal of Rock Mechanics and Geotechnical Engineering, 7(2), pp.213-219.

Gilmullina, A., Klausen, T.G., Paterson, N.W., Suslova, A. and Eide, C.H., 2021. Regional correlation and seismic stratigraphy of Triassic Strata in the Greater Barents Sea: Implications for sediment transport in Arctic basins. Basin Research, 33(2), pp.1546-1579.

Green, P.F. and Japsen, P., 2018. Burial and exhumation history of the Jameson Land Basin, East Greenland, estimated from thermochronological data from the Blokelv-1 core. Geological Survey of Denmark and Greenland Bulletin, pp.133-147.

Guarnieri, P., Brethes, A. and Rasmussen, T.M., 2017. Geometry and kinematics of the Triassic rift basin in Jameson Land (East Greenland). Tectonics, 36(4), pp.602-614.

Gudmundsson, A., 1990. Emplacement of dikes, sills and crustal magma chambers at divergent plate boundaries. Tectonophysics, 176(3-4), pp.257-275.

Gudmundsson, A., 2006. How local stresses control magma-chamber ruptures, dyke injections, and eruptions in composite volcanoes. Earth-Science Reviews, 79(1-2), pp.1-31.

Hafeez, A., Planke, S., Jerram, D.A., Millett, J.M., Maharjan, D., Prestvik, T., 2017. Upper Paleocene ultramafic igneous rocks offshore Mid-Norway: re-interpretation of the Vestbrona Formation as a sill complex. AAPG Interpretation, 5(3), SK103-SK120.

Hald, N. and Tegner, C., 2000. Composition and age of tertiary sills and dykes, Jameson Land Basin, East Greenland: relation to regional flood volcanism. Lithos, 54(3-4), pp.207-233.

Hansen, J., D.A. Jerram, K. McCaffrey, S.R. Passey; Early Cenozoic saucer-shaped sills of the Faroe Islands: an example of intrusive styles in basaltic lava piles. Journal of the Geological Society 2011;; 168 (1): 159–178. doi: https://doi.org/10.1144/0016-76492010-012

Hansen, J., Jerram, D.A., McCaffrey, K. and Passey, S.R., 2009. The onset of the North Atlantic Igneous Province in a rifting perspective. Geological Magazine, 146(3), pp.309-325.

Hansen, K., Bergman, S.C. and Henk, B., 2001. The Jameson Land basin (east Greenland): a fission track study of the tectonic and thermal evolution in the Cenozoic North Atlantic spreading regime. Tectonophysics, 331(3), pp.307-339.

Hayman, P.C., Campbell, I.H., Cas, R.A.F., Squire, R.J., Doutch, D. and Outhwaite, M., 2021. Differentiated Archean Dolerites: Igneous and Emplacement Processes that Enhance Prospectivity for Orogenic Gold. Economic Geology.

Holness, M.B., Nielsen, T.F. and Tegner, C., 2017. The Skaergaard intrusion of East Greenland: paradigms, problems and new perspectives. Elements: An International Magazine of Mineralogy, Geochemistry, and Petrology, 13(6), pp.391-396.

Hopper J.R. Dahl-Jensen T. Holbrook W.S. Larsen H.C. Lizarralde D. Korenaga J. Kent G.M. Kelemen P.B. , 2003. Structure of the SE Greenland margin from seismic reflection and refraction data:

implications for nascent spreading center subsidence and asymmetric crustal accretion during North Atlantic opening, J. Geophys. Res., 108 (B5), 2269.

Horni, J.Á., Hopper, J.R., Blischke, A., Geisler, W.H., Stewart, M., McDermott, K., Judge, M., Erlendsson, Ö. and Árting, U., 2017. Regional distribution of volcanism within the North Atlantic Igneous Province. Geological Society, London, Special Publications, 447(1), pp.105-125.

Huang, H.H., Lin, F.C., Schmandt, B., Farrell, J., Smith, R.B. and Tsai, V.C., 2015. The Yellowstone magmatic system from the mantle plume to the upper crust. Science, 348(6236), pp.773-776.

Jackson, M.D. and Pollard, D.D., 1988. The laccolith-stock controversy: New results from the southern Henry Mountains, Utah. Geological Society of America Bulletin, 100(1), pp.117-139.

Jaxybulatov, K., Shapiro, N.M., Koulakov, I., Mordret, A., Landès, M. and Sens-Schönfelder, C., 2014. A large magmatic sill complex beneath the Toba caldera. science, 346(6209), pp.617-619.

Jerram D.A., Bryan S.E. (2015) Plumbing Systems of Shallow Level Intrusive Complexes. In: Breitkreuz C., Rocchi S. (eds) Physical Geology of Shallow Magmatic Systems. Advances in Volcanology (An Official Book Series of the International Association of Volcanology and Chemistry of the Earth's Interior). Springer, Cham. Pp 39-60. https://doi.org/10.1007/11157_2015_8

Jerram, D. A., Davis, G. R., Mock, A., Charrier, A., Marsh, B. D., 2010. Quantifying 3D crystal populations, packing and layering in shallow intrusions: A case study from the Basement Sill, Dry Valleys, Antarctica. Geosphere 2010;; 6 (5): 537–548. doi: https://doi.org/10.1130/GES00538.1

Kavanagh, J.L., Rogers, B.D., Boutelier, D. and Cruden, A.R., 2017. Controls on sill and dyke-sill hybrid geometry and propagation in the crust: The role of fracture toughness. Tectonophysics, 698, pp.109-120.

Kilhams, B., Lauren Chedburn, Nick Schofield, Ingelin Løkling Lunde, Hollie Romain, David Jolley & Christian Haug Eide, 2021. Igneous Centres along the Norwegian Atlantic Margin (Møre and Vøring) and their relationship to magmatic plumbing systems, Journal of the Geological Society, DOI: https://doi.org/10.1144/jgs2020-192

Kjøll, H.J., Galland, O., Labrousse, L. and Andersen, T.B., 2019. Emplacement mechanisms of a dyke swarm across the brittle-ductile transition and the geodynamic implications for magma-rich margins. Earth and Planetary Science Letters, 518, pp.223-235.

Larsen, H.C. and Marcussen, C., 1992. Sill-intrusion, flood basalt emplacement and deep crustal structure of the Scoresby Sund region, East Greenland. Geological Society, London, Special Publications, 68(1), pp.365-386.

Larsen, L.M., 2018. Igneous intrusions in the cored Upper Jurassic succession of the Blokelv-1 borehole, Jameson Land Basin, East Greenland. Geological Survey of Denmark and Greenland Bulletin, pp.127-131.

Larsen, L.M., Pedersen, A.K., Tegner, C. and Duncan, R.A., 2014. Eocene to Miocene igneous activity in NE Greenland: northward younging of magmatism along the East Greenland margin. Journal of the Geological Society, 171(4), pp.539-553.

Lecomte, I., Lavadera, P.L., Botter, C., Anell, I., Buckley, S.J., Eide, C.H., Grippa, A., Mascolo, V. and Kjoberg, S., 2016. 2 (3) D convolution modelling of complex geological targets beyond–1D convolution. First Break, 34(5).

Lorenz, V. and Haneke, J., 2004. Relationship between diatremes, dykes, sills, laccoliths, intrusive-extrusive domes, lava flows, and tephra deposits with unconsolidated water-saturated sediments in the late Variscan intermontane Saar-Nahe Basin, SW Germany. Geological Society, London, Special Publications, 234(1), pp.75-124.

MacDonald, A.M., Davies, J. and Peart, R.J., 2001. Geophysical methods for locating groundwater in low permeability sedimentary rocks: examples from southeast Nigeria. Journal of African Earth Sciences, 32(1), pp.115-131.

Magee, C. and Jackson, C.A.L., 2020. Seismic reflection data reveal the 3D structure of the newly discovered Exmouth Dyke Swarm, offshore NW Australia. Solid Earth, 11(2), pp.579-606.

Magee, C., Bastow, I.D., van Wyk de Vries, B., Jackson, C.A.L., Hetherington, R., Hagos, M. and Hoggett, M., 2017. Structure and dynamics of surface uplift induced by incremental sill emplacement. Geology, 45(5), pp.431-434.

Magee, C., Ernst, R.E., Muirhead, J., Phillips, T. and Jackson, C.A.L., 2019. Magma transport pathways in large igneous provinces: lessons from combining field observations and seismic reflection data. In Dyke Swarms of the World: A Modern Perspective (pp. 45-85). Springer, Singapore.

Magee, C., Jackson, C.A.L., Hardman, J.P. and Reeve, M.T., 2017. Decoding sill emplacement and forced fold growth in the Exmouth Sub-basin, offshore northwest Australia: Implications for hydrocarbon exploration. Interpretation, 5(3), pp.SK11-SK22.

Magee, C., Muirhead, J.D., Karvelas, A., Holford, S.P., Jackson, C.A., Bastow, I.D., Schofield, N., Stevenson, C.T., McLean, C., McCarthy, W. and Shtukert, O., 2016. Lateral magma flow in mafic sill complexes. Geosphere, 12(3), pp.809-841.

Mandler, H.A. and Jokat, W., 1998. The crustal structure of Central East Greenland: results from combined land-sea seismic refraction experiments. Geophysical Journal International, 135(1), pp.63-76.

Mark, N.J., Schofield, N., Pugliese, S., Watson, D., Holford, S., Muirhead, D., Brown, R. and Healy, D., 2018. Igneous intrusions in the Faroe Shetland basin and their implications for hydrocarbon exploration; new insights from well and seismic data. Marine and Petroleum Geology, 92, pp.733-753.

Mathiesen, A., Bidstrup, T. and Christiansen, F.G., 2000. Denudation and uplift history of the Jameson Land basin, East Greenland—constrained from maturity and apatite fission track data. Global and Planetary Change, 24(3-4), pp.275-301.

Minakov, A., Yarushina, V., Faleide, J.I., Krupnova, N., Sakoulina, T., Dergunov, N. and Glebovsky, V., 2018. Dyke emplacement and crustal structure within a continental large igneous province, northern Barents Sea. Geological Society, London, Special Publications, 460(1), pp.371-395.

Mjelde, R., Raum, T., Breivik, A.J. and Faleide, J.I., 2008. Crustal transect across the North Atlantic. Marine Geophysical Researches, 29(2), p.73.

Monreal, F.R., Villar, H.J., Baudino, R., Delpino, D. and Zencich, S., 2009. Modeling an atypical petroleum system: A case study of hydrocarbon generation, migration and accumulation related to igneous intrusions in the Neuquen Basin, Argentina. Marine and Petroleum Geology, 26(4), pp.590-605.

Muirhead, J.D., Airoldi, G., White, J.D. and Rowland, J.V., 2014. Cracking the lid: Sill-fed dikes are the likely feeders of flood basalt eruptions. Earth and Planetary Science Letters, 406, pp.187-197.

Neumann, E.R., Svensen, H., Tegner, C., Planke, S., Thirlwall, M. and Jarvis, K.E., 2013. Sill and lava geochemistry of the mid-Norway and NE Greenland conjugate margins. Geochemistry, Geophysics, Geosystems, 14(9), pp.3666-3690.

Noe-Nygaard, A. (1976) Tertiary igneous rocks between Shannon and Scoresby Sund East Greenland. In: Geology of Greenland (Eds A. Escher and W. S. Watt) Grønlands Geologiske Undersøgelse, 386-402

Parsons, A.J., Whitham, A.G., Kelly, S.R.A., Vautravers, B.P.H., Dalton, T.J.S., Andrews, S.D., Pickles, C.S., Strogen, D.P., Braham, W., Jolley, D.W. and Gregory, F.J., 2017. Structural evolution and basin architecture of the Traill Ø region, NE Greenland: A record of polyphase rifting of the East Greenland continental margin. Geosphere, 13(3), pp.733-770.

Pedersen, M., Weng, W.L., Keulen, N. and Kokfelt, T.F., 2013. A new seamless digital 1: 500 000 scale geological map of Greenland. Geological Survey of Denmark and Greenland (GEUS) Bulletin, 28, pp.65-68.

Pedersen, R. and Sigmundsson, F., 2004. InSAR based sill model links spatially offset areas of deformation and seismicity for the 1994 unrest episode at Eyjafjallajökull volcano, Iceland. Geophysical Research Letters, 31(14).

Planke S., Svensen H., Myklebust R., Bannister S., Manton B., Lorenz L. (2015) Geophysics and Remote Sensing. In: Breitkreuz C., Rocchi S. (eds) Physical Geology of Shallow Magmatic Systems. Advances in Volcanology (An Official Book Series of the International Association of Volcanology and Chemistry of the Earth's Interior). Springer, Cham. https://doi.org/10.1007/11157_2014_6Saunders, A. D., Fitton, J. G., Kerr, A. C., Norry, M. J. and Kent, R. W. 1997. The North Atlantic Igneous Province. Geophysical Monograph 100, 45–93.

Polteau, S., Mazzini, A., Galland, O., Planke, S., and Malthe-Sørenssen, A., 2008a, Saucer-shaped intrusions: Occurrences, emplacement and implications: Earth and Planetary Science Let-ters, v. 266, p. 195–204, doi: 10 .1016 /j .epsl .2007 .11 .015

Poppe, S., Galland, O., de Winter, N.J., Goderis, S., Claeys, P., Debaille, V., Boulvais, P. and Kervyn, M., 2020. Structural and geochemical interactions between magma and sedimentary host rock: The Hovedøya case, Oslo Rift, Norway. Geochemistry, Geophysics, Geosystems, 21(3), p.e2019GC008685.

Schofield, N., Jerram, D.A., Holford, S., Archer, S., Mark, N., Hartley, A., Howell, J., Muirhead, D., Green, P., Hutton, D., and Stevenson, C., 2016, Sills in sedimentary basins and petroleum systems, in Breitkreuz, C. and Rocchi, S., eds., Physical Geology of Shallow Magmatic Systems: Dykes, Sills and Laccoliths: Cham, Switzerland, Springer, p. 273–294, https:// doi .org /10 .1007 /11157_2015_17.

Schofield, N., Jolley, D., Holford, S., Archer, S., Watson, D., Hartley, A., Howell, J., Muirhead, D., Underhill, J. and Green, P., 2018, January. Challenges of future exploration within the UK Rockall Basin. In Geological Society, London, Petroleum Geology Conference series (Vol. 8, No. 1, pp. 211-229). Geological Society of London.

Schofield, N., Holford, S., Millett, J., Brown, D., Jolley, D., Passey, S.R., Muirhead, D., Grove, C., Magee, C., Murray, J. and Hole, M., 2017. Regional magma plumbing and emplacement mechanisms of the Faroe-Shetland Sill Complex: implications for magma transport and petroleum systems within sedimentary basins. Basin Research, 29(1), pp.41-63.

Schofield, N.J., Brown, D.J., Magee, C. and Stevenson, C.T., 2012. Sill morphology and comparison of brittle and non-brittle emplacement mechanisms. Journal of the Geological Society, 169(2), pp.127-141.

Senger, K., Millett, J., Planke, S., Ogata, K., Eide, C.H., Festøy, M., Galland, O. and Jerram, D.A., 2017. Effects of igneous intrusions on the petroleum system: a review. First Break, 35(6), pp.47-56.

Shaw, H.R., Wright, T.L., Peck, D.L. and Okamura, R., 1968. The viscosity of basaltic magma; an analysis of field measurements in Makaopuhi lava lake, Hawaii. American Journal of Science, 266(4), pp.225-264.

Sigmundsson, F., Hreinsdóttir, S., Hooper, A., Árnadóttir, T., Pedersen, R., Roberts, M.J., Óskarsson, N., Auriac, A., Decriem, J., Einarsson, P. and Geirsson, H., 2010. Intrusion triggering of the 2010 Eyjafjallajökull explosive eruption. Nature, 468(7322), p.426.

Stephens, T.L., Walker, R.J., Healy, D., Bubeck, A., England, R.W. and McCaffrey, K.J., 2017. Igneous sills record far-field and near-field stress interactions during volcano construction: Isle of Mull, Scotland. Earth and Planetary Science Letters, 478, pp.159-174.

Surlyk, F., Callomon, J.H., Bromley, R.G. and Birkelund, T., 1973. Stratigraphy of the Jurassic-Lower Cretaceous sediments of Jameson Land and Scoresby Land, East Greenland. Copenhagen: Bianco Lunas Bogtrykkeri.

Svensen Henrik H., Frolov Sergei, Akhmanov Grigorii G., Polozov Alexander G., Jerram Dougal A., Shiganova Olga V., Melnikov Nikolay V., Iyer Karthik and Planke Sverre, 2018. Sills and gas generation in the Siberian Traps. Phil. Trans. R. Soc. A.37620170080http://doi.org/10.1098/rsta.2017.0080

Svensen, H.H., Polteau, S., Cawthorn, G. and Planke, S., 2014. Sub-volcanic intrusions in the Karoo basin, South Africa. In Physical geology of shallow magmatic systems (pp. 349-362). Springer, Cham.

Talwani, M. and Eldholm, O., 1977. Evolution of the Norwegian-Greenland sea. Geological Society of America Bulletin, 88(7), pp.969-999.

Thybo, H. and Artemieva, I.M., 2013. Moho and magmatic underplating in continental lithosphere. Tectonophysics, 609, pp.605-619.

Voss, M,. Jokat, W., Continent-ocean transition and voluminous magmatic underplating derived from P-wave velocity modelling of the East Greenland continental margin, Geophysical Journal International, Volume 170, Issue 2, August 2007, Pages 580–604, https://doi.org/10.1111/j.1365-246X.2007.03438.x

Voss, M., Schmidt-Aursch, M.C. and Jokat, W., 2009. Variations in magmatic processes along the East Greenland volcanic margin. Geophysical Journal International, 177(2), pp.755-782.

Wada, Y., 1994. On the relationship between dike width and magma viscosity. Journal of Geophysical Research: Solid Earth, 99(B9), pp.17743-17755.

Walker, F., Schofield, N., Millett, J., Jolley, D., Holford, S., Planke, S., Jerram, D.A. and Myklebust, R., 2021. Inside the volcano: Three-dimensional magmatic architecture of a buried shield volcano. Geology, 49(3), pp.243-247.

Walker, R.J. and Gill, S.P.A., 2020. Tectonic stress controls saucer-shaped sill geometry and emplacement mechanism. Geology, 48(9), pp.898-902.

Walker, R.J., Healy, D., Kawanzaruwa, T.M., Wright, K.A., England, R.W., McCaffrey, K.J.W., Bubeck, A.A., Stephens, T.L., Farrell, N.J.C. and Blenkinsop, T.G., 2017. Igneous sills as a record of horizontal shortening: The San Rafael subvolcanic field, Utah. GSA Bulletin, 129(9-10), pp.1052-1070.

Wall, M., Cartwright, J., Davies, R. and McGrandle, A., 2010. 3D seismic imaging of a Tertiary Dyke Swarm in the Southern North Sea, UK. Basin Research, 22(2), pp.181-194.

Weigel, W., Flüh, E.R., Miller, H., Butzke, A., Dehghani, G.A., Gebhardt, V., Harder, I., Hepper, J., Jokat, W., Kläschen, D. and Kreymann, S., 1995. Investigations of the East Greenland continental margin between 70 and 72 N by deep seismic sounding and gravity studies. Marine Geophysical Researches, 17(2), pp.167-199.

Widess, M.B., 1973. How thin is a thin bed?. Geophysics, 38(6), pp.1176-1180.

Wrona, T., Magee, C., Fossen, H., Gawthorpe, R.L., Bell, R.E., Jackson, C.L. and Faleide, J.I., 2019. 3-D seismic images of an extensive igneous sill in the lower crust. Geology, 47(8), pp.729-733.

Ziolkowski, A., Hanssen, P., Gatliff, R., Jakubowicz, H., Dobson, A., Hampson, G., Li, X.Y. and Liu, E., 2003. Use of low frequencies for sub-basalt imaging. Geophysical Prospecting, 51(3), pp.169-182.

11. Appendix

DR1: Uninterpreted and un-warped version of seismic line in Fig. 4.

DR2: Spreadsheet showing thickness of sills and width of dykes in study area.

DR3: Assumptions and calculations of magma volume in southern Sill Complex in Jameson land Basin.

Figure 1

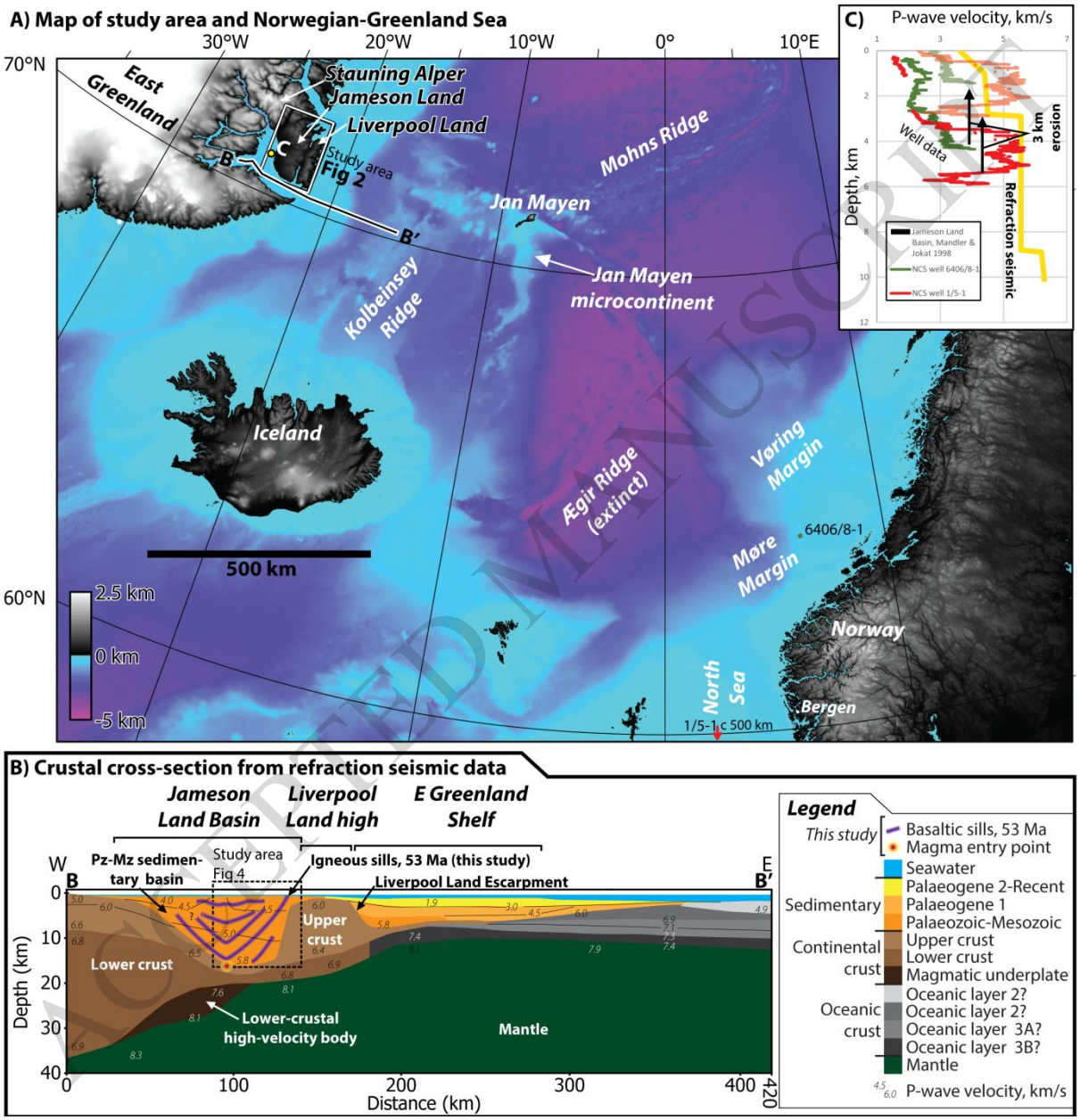

Figure 2

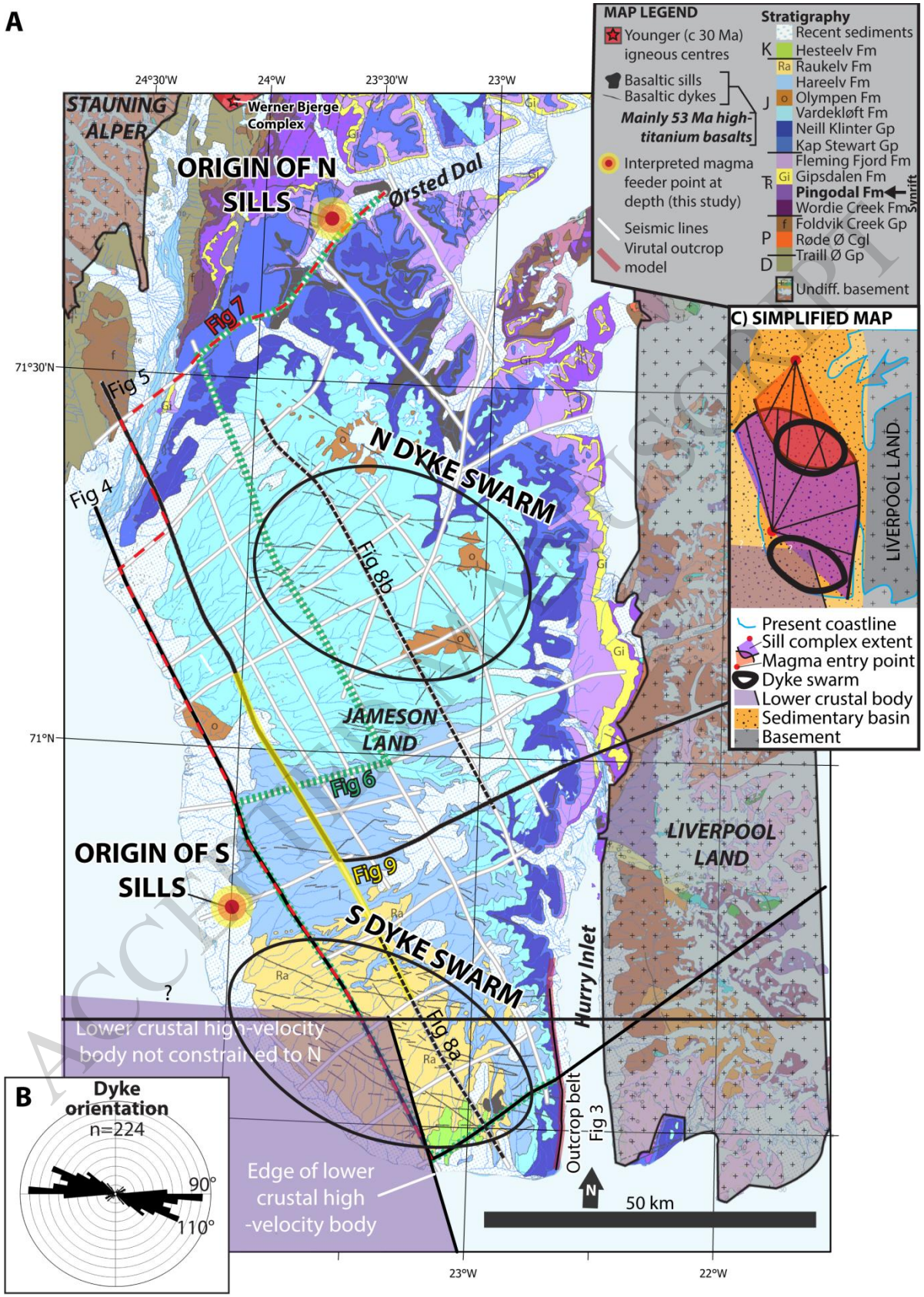

Figure 3

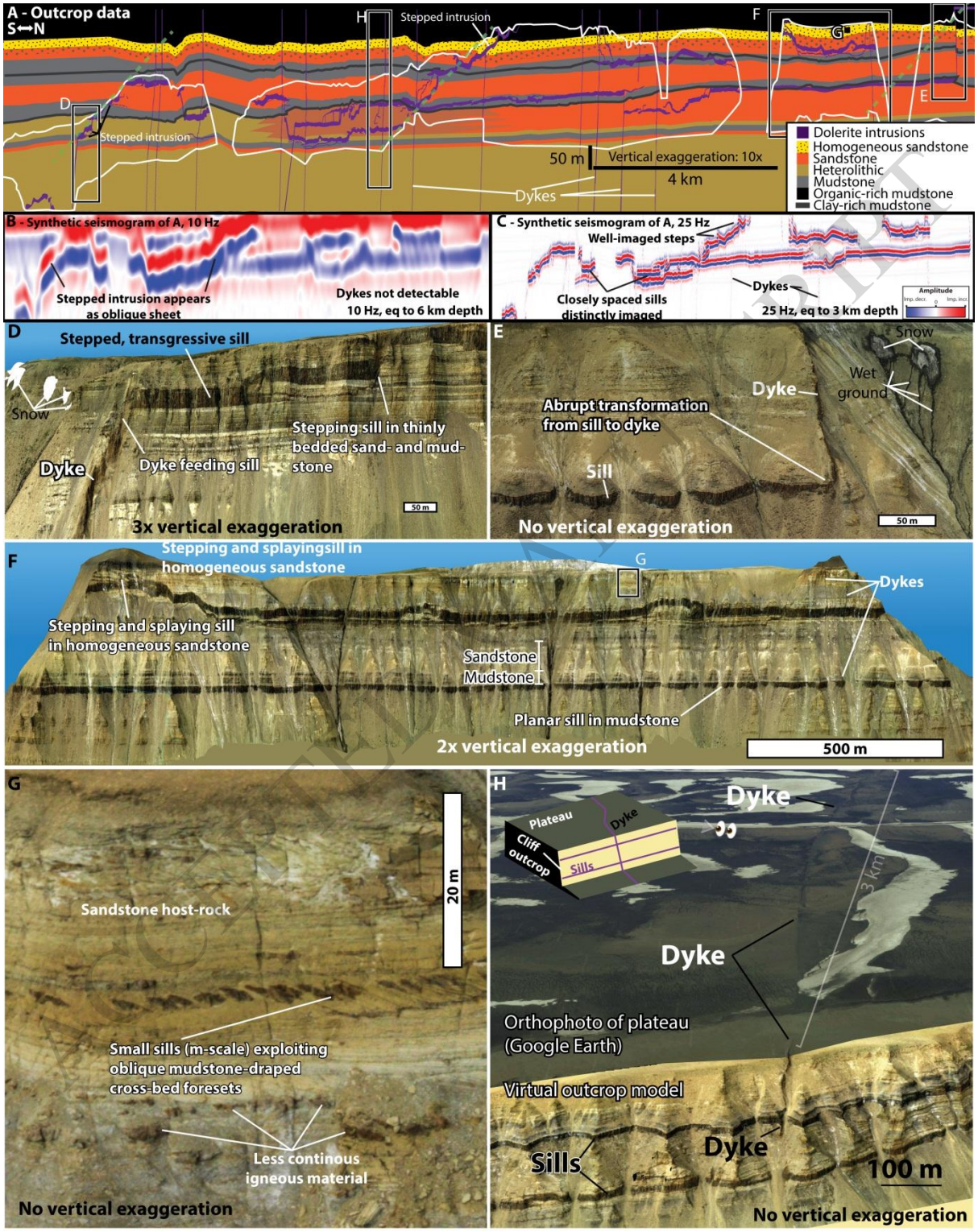

Figure 4

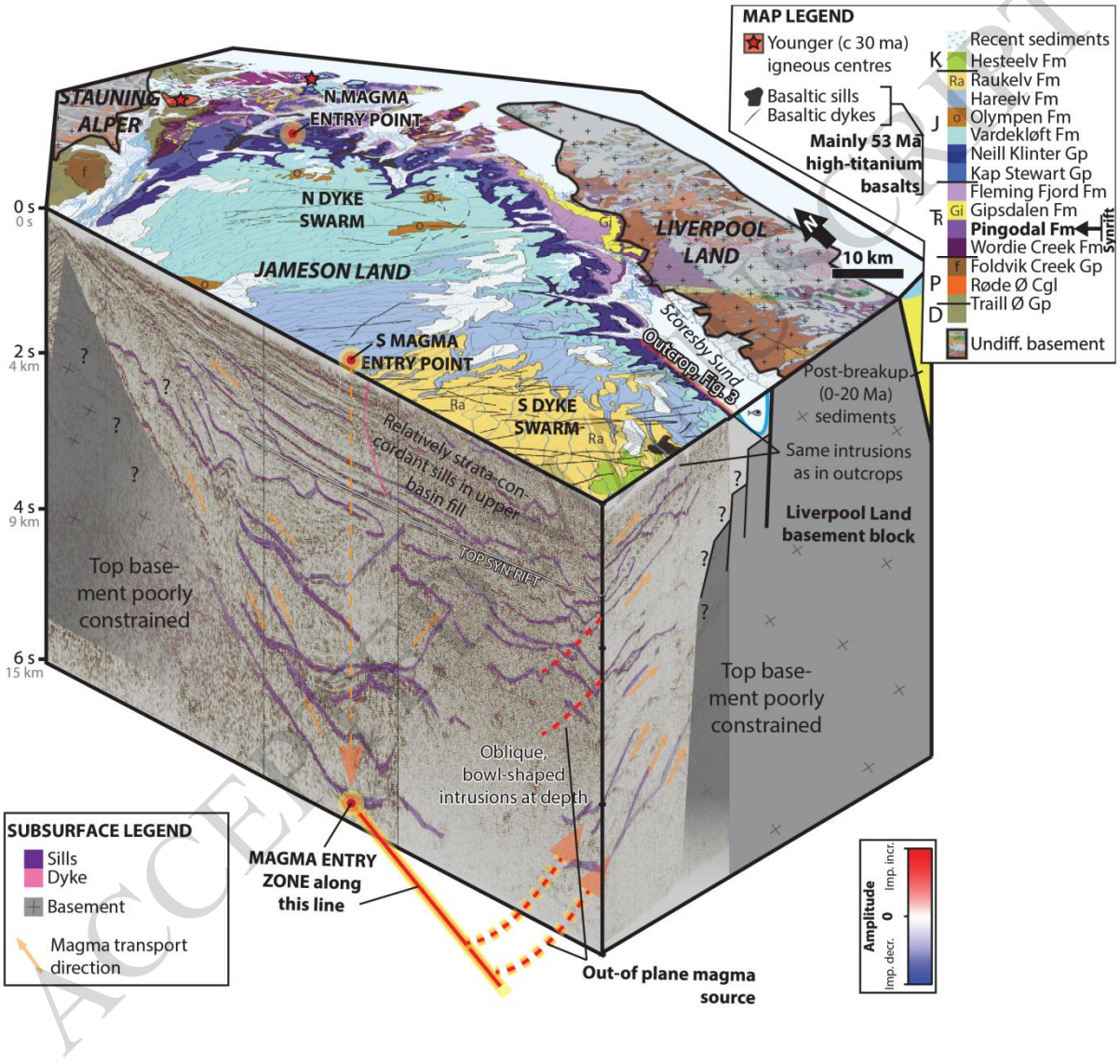

Figure 5

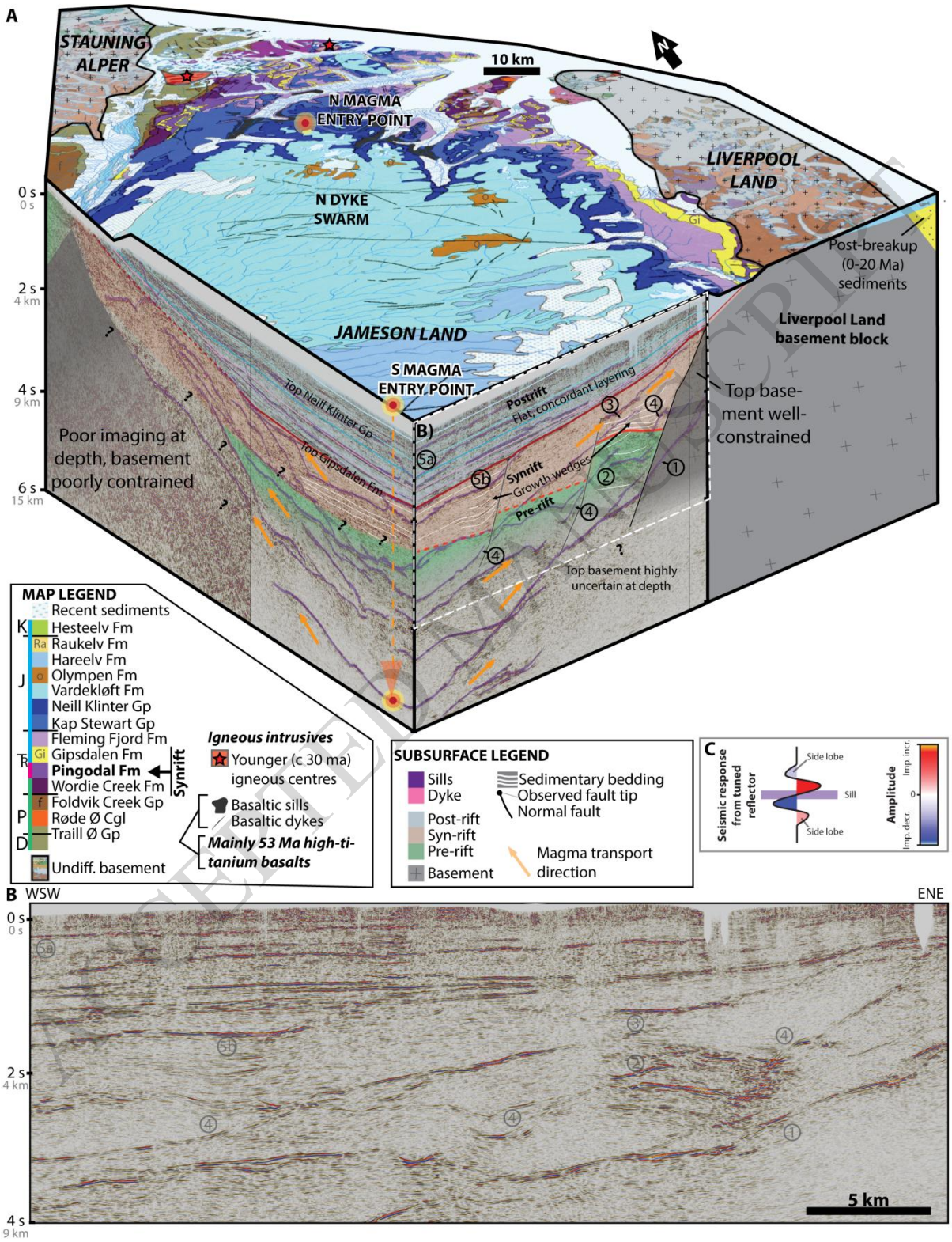

Figure 6

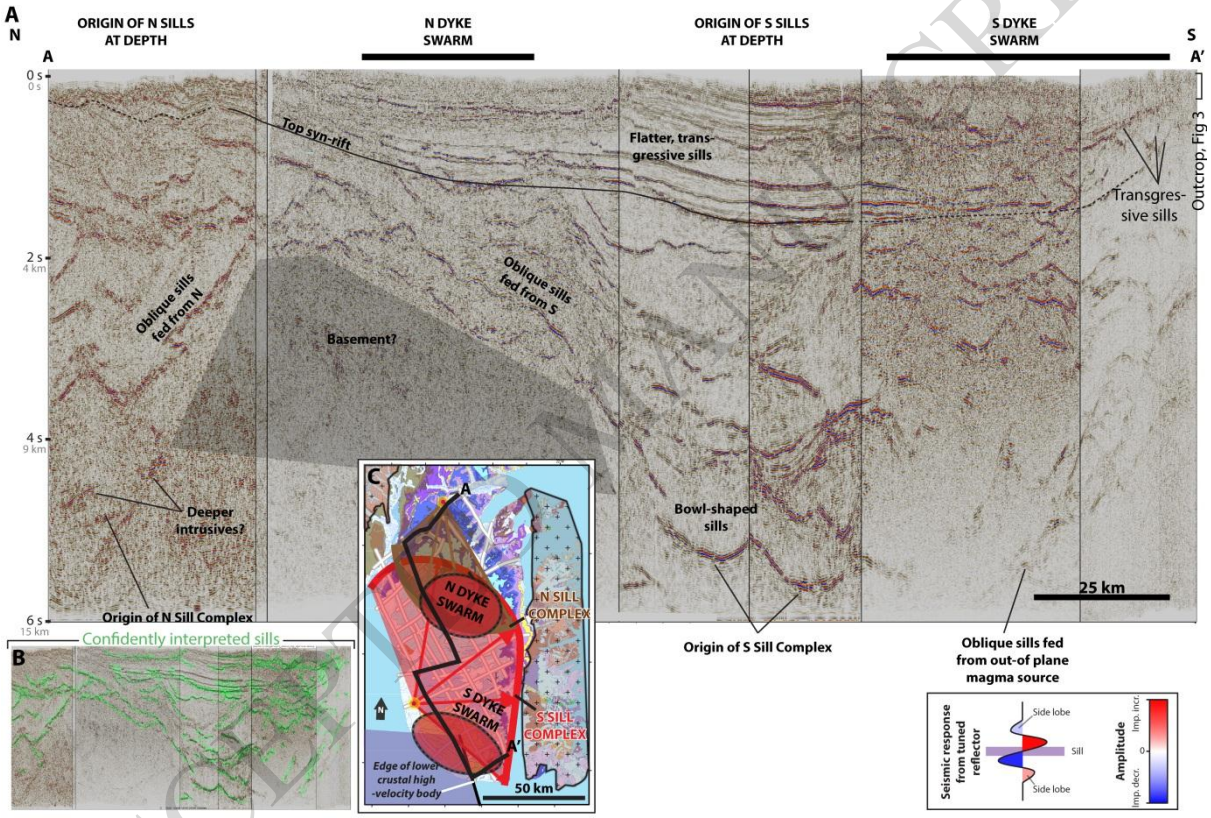

Figure 7

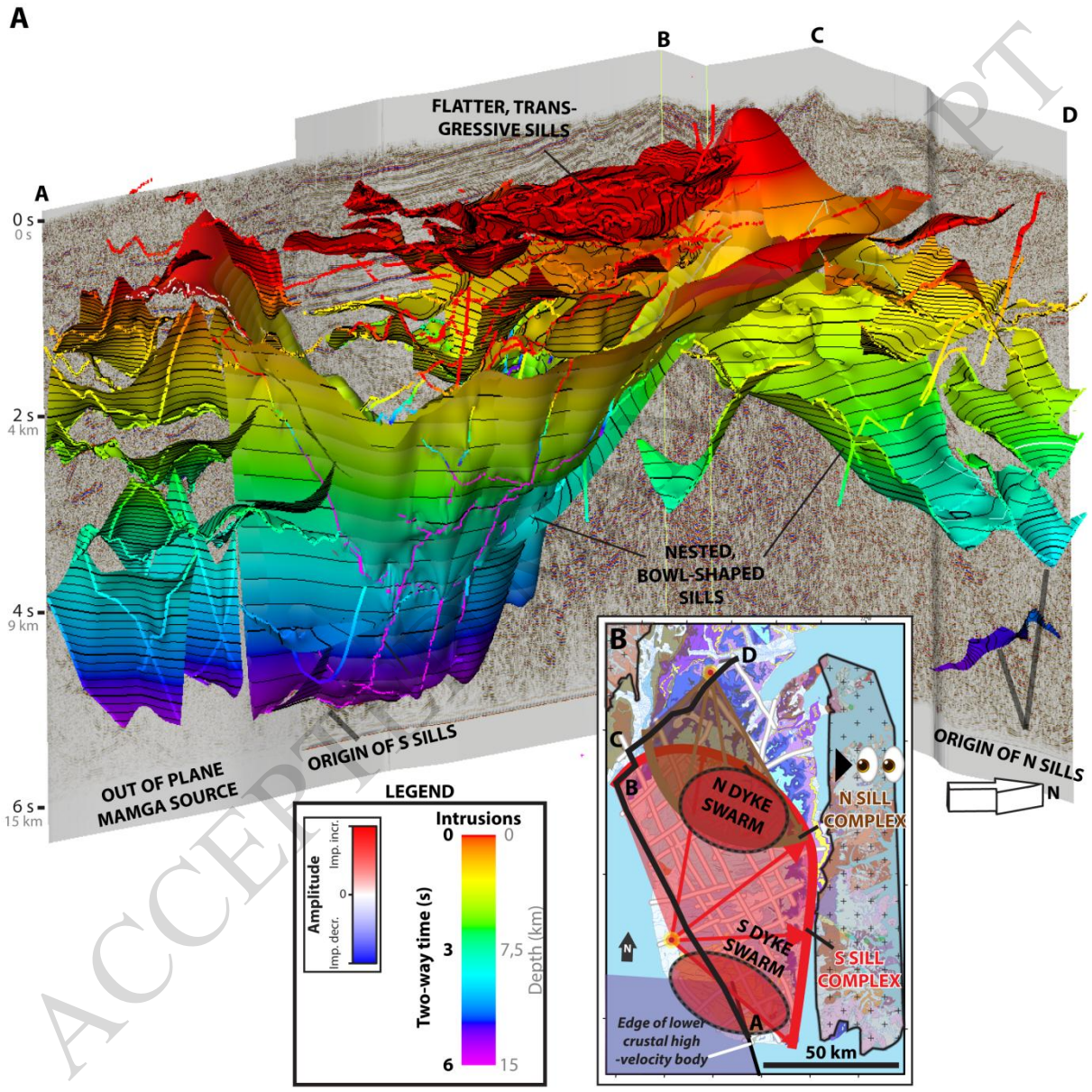

Figure 8

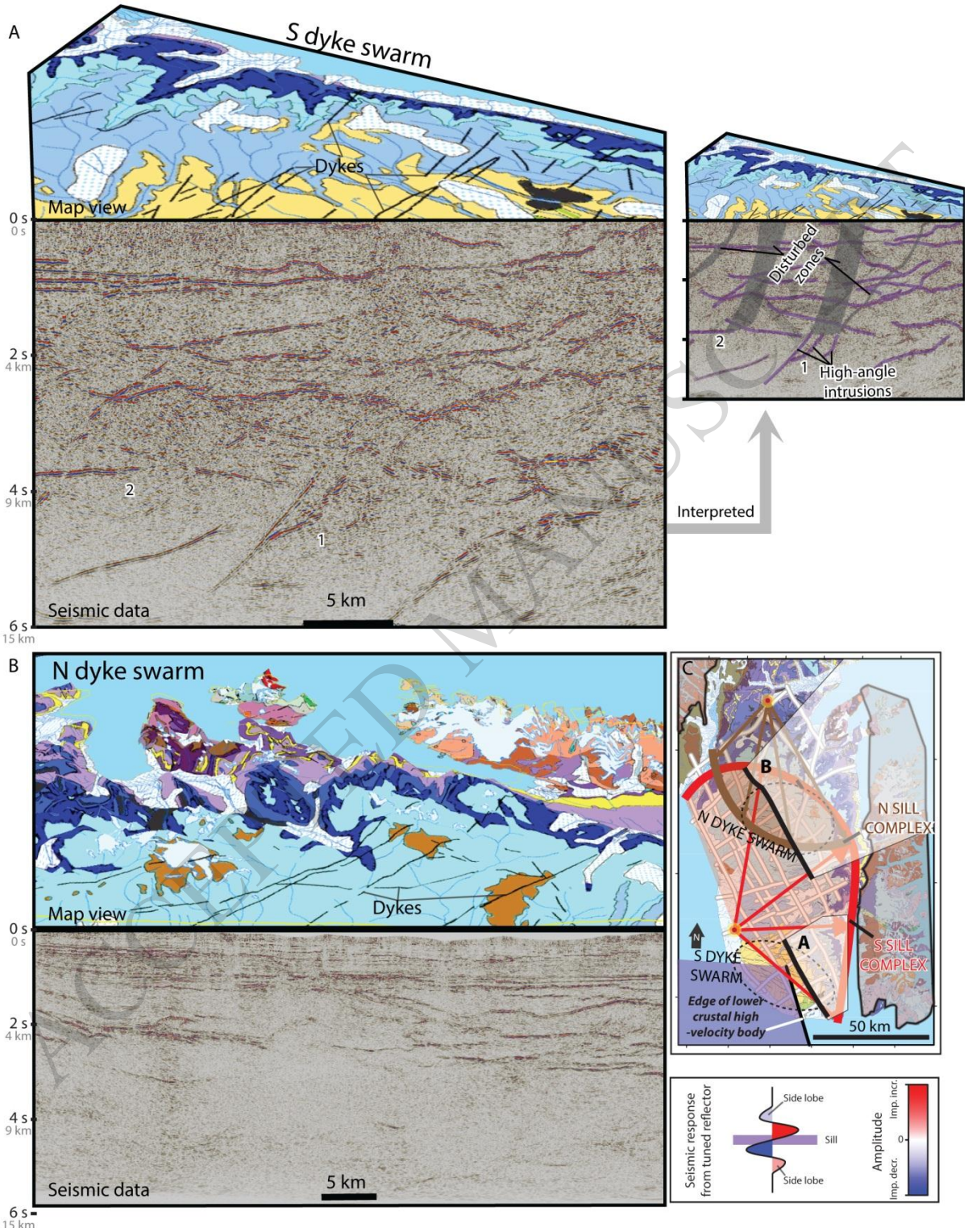

Figure 9

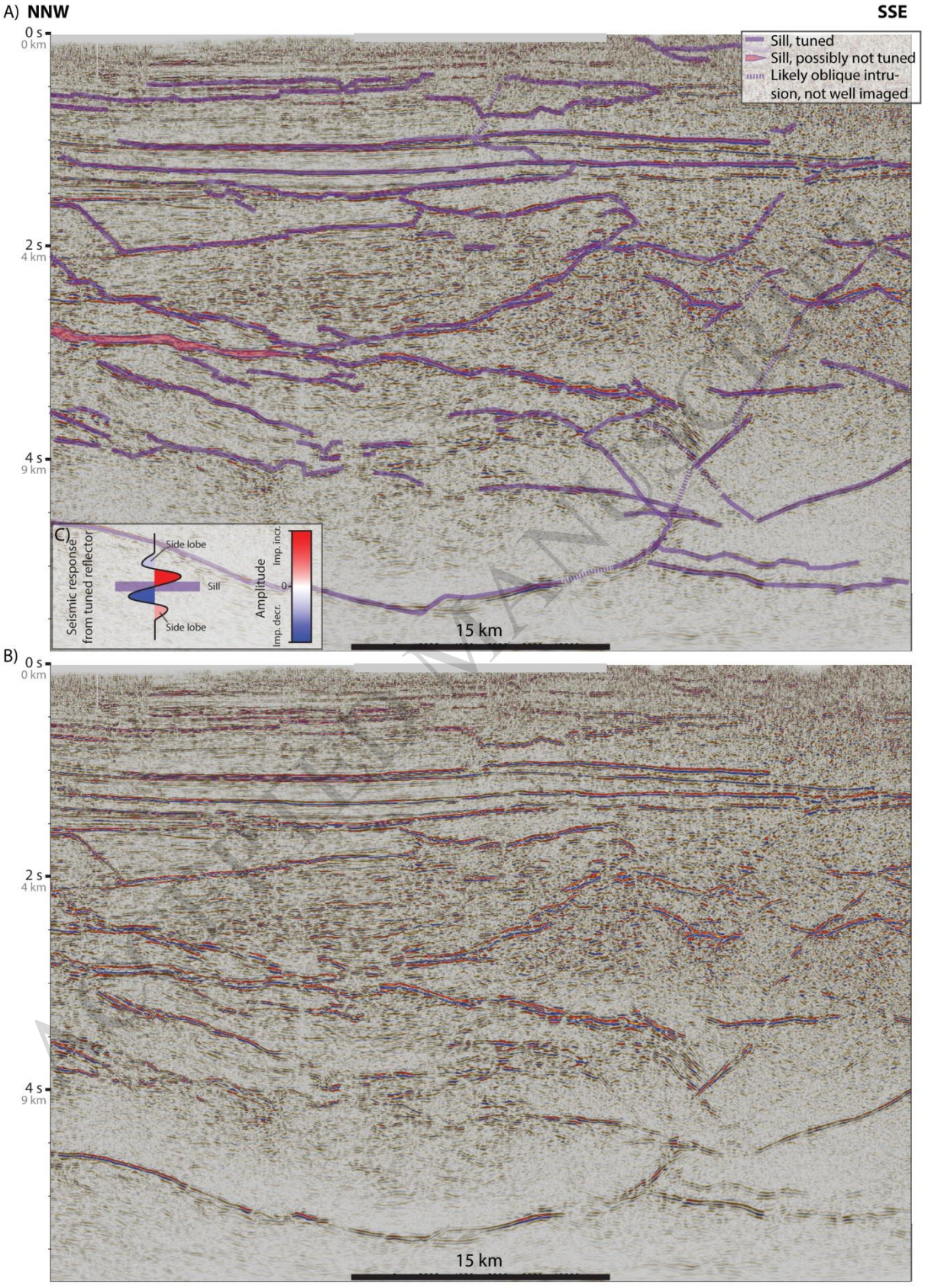

Figure 10

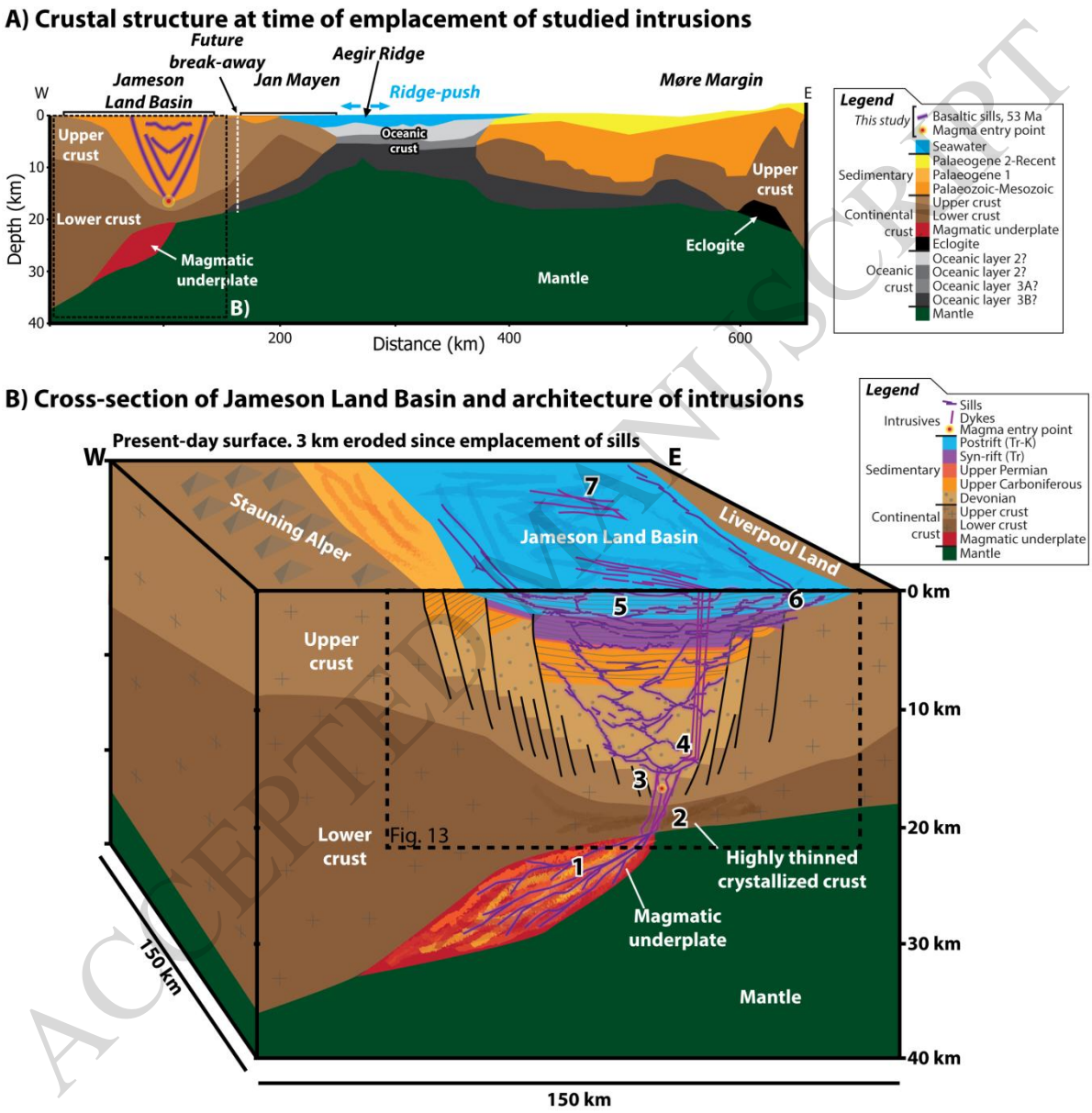

Figure 11

Figure 12

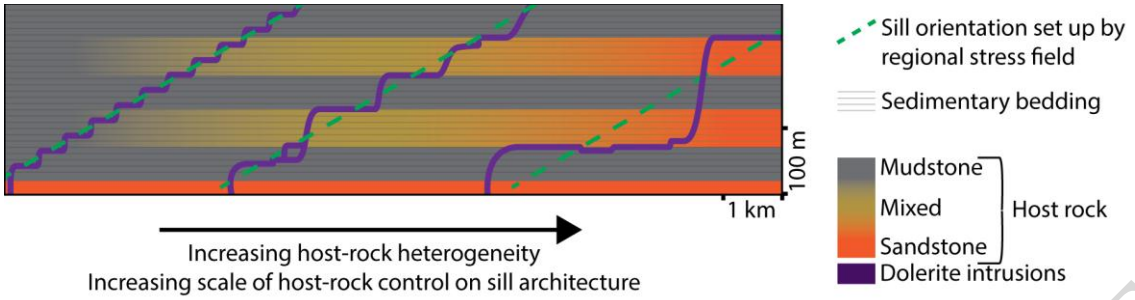

Figure 13